LAPPEENRANTA UNIVERSITY OF TECHNOLOGY

LUT School of Energy Systems

Master of Science in Bioenergy Technology

Hoang Si Huy Nguyen

GREEN DIESEL SYNTHESIS BY HYDRODEOXYGENATION OF LIPIDS EXTRACTED FROM *CHLORELLA* ALGAE IN SUPERCRITICAL HEXANE

Examiners: Professor Esa K. Vakkilainen

Professor Dmitry Yu. Murzin

ABSTRACT

LAPPEENRANTA UNIVERSITY OF TECHNOLOGY

LUT School of Energy Systems

Bioenergy Technology

Hoang Si Huy Nguyen

Green diesel synthesis by hydrodeoxygenation of lipids extracted from *Chlorella* algae in supercritical hexane

Master's thesis

2016

64 pages, 21 figures, 9 tables and 2 appendices

Examiners Professor, D.Sc. Esa K. Vakkilainen (LUT)

Professor, D.Sc. Dmitry Yu. Murzin (Åbo Akademi University)

Supervisors Professor, D.Sc. Esa K. Vakkilainen (LUT)

Professor, D.Sc. Dmitry Yu. Murzin (Åbo Akademi University)

Docent Päivi Mäki-Arvela (Åbo Akademi University)

Lipids were extracted from *Chlorella* algae with supercritical hexane. The high lipids yield of approximately 10% was obtained at optimum conditions of 300 rpm stirring speed and 2 h duration compared to the total contents of lipids being 12%. Furthermore, an easiness of hexane recovery may be considered as economically and ecologically attractive. For the first time, in the current work catalytic hydrodeoxygenation (HDO) of *Chlorella* algal lipids was studied over 5 wt% Ni/H-Y-80 and 5 wt% Ni/SiO_2 at 300 °C and under 30 bar total pressure in H_2. A comparative HDO of stearic acid was carried out under similar conditions. The conversion of lipids was about 35% over 5 wt% Ni/H-Y-80 after 6h, whereas, 5 wt% Ni/SiO_2 was totally deactivated after 60 min. The selectivity to hydrocarbons (C15-C18) is 6%. As a comparison, complete conversion of stearic acid over 5 wt% Ni/H-Y-80 was achieved in 6 h. The transformation of lipids proceeded mostly via hydrogenation and hydrolysis with formation of free fatty acid (FFA). The lower activity might be attributed to deactivation of catalysts caused by chlorophylls and carotenoids. Even though the conversion is low, future studies in HDO of lipids extracted from other algae species having higher lipid content could be proposed. Coke resistant catalyst might be considered to improve catalytic activity.

ACKNOWLEDGEMENT

First of all, I would like to express my gratitude to Professor Esa K. Vakkilainen for supporting me to work at Laboratory of Industrial Chemistry and Reaction Engineering at Åbo Akademi University. In addition, I have received his guidance and advice for my work.

Secondly, I am also deeply grateful to Professor Dmitry Yu. Murzin for his allowance to carry out my research in Laboratory of Industrial Chemistry and Reaction Engineering. It is my honor to work with him who has given useful information and intelligence during my work.

Furthermore, Docent Päivi Mäki-Arvela deserves my endless gratefulness for her kind support from the beginning of my work. Whenever I had difficulties, she was so eager to help me, without her help my thesis could not be possible. I have learnt a lot of valuable know-how during working with her.

I would like to thank our laboratory manager Docent Kari Eränen in Laboratory of Industrial Chemistry and Reaction Engineering for his technical support. The problems were easily figured out by his skillfulness, to Imane Hachemi for her guidance and time to help me to get familiar with hydrodeoxygenation experiments.

I also could not forget the help of Dr. Annika Smeds, Jarl Hemming, Peter Backman, Linus Silvander, Atte Aho and Sten Lindhom in Johan Gadolin Process Chemistry Centre (PCC) for their support and guidance in measurements and Markus Peurla in University of Turku for his performance of transmission electron microscopy. My gratitude also goes to Andre Rudnäs, a student at Åbo Akademi University, whom I supervised.

Last but not least, I would like to thank my family and my girlfriend Trinh who have fully supported me not only during my study but also in my life.

Lappeenranta, May 2016

Hoang S. H. Nguyen

TABLE OF CONTENTS

ABSTRACT 2

ACKNOWLEDGEMENT 3

LIST OF ABBREVIATIONS 7

1 INTRODUCTION 9

1.1 Feedstock 10

1.2 Biorefinery 12

1.3 Cell disruption and lipid extraction 12

1.4 Biodiesel production 13

1.5 Green diesel production 14

1.6 Catalysts 15

1.6.1 Zeolite as catalysts and supports 16

1.6.2 Metal as active site for (hydro)deoxygenation reaction 17

1.7 Characterization techniques 18

1.7.1 N_2 physisorption 18

1.7.2 Temperature programmed techniques 20

1.7.3 Electron microscopy 21

1.8 Analysis of liquid phase 22

1.8.1 Gas chromatography 22

1.8.2 Gas chromatography/flame ionization detector (GC-FID) 22

1.8.3 Gas chromatography/mass spectrometry (GC-MS) 23

1.8.4 Principle of internal standard method 23

1.8.5 Validation of the method 24

1.9 UV-Vis spectroscopy 24

1.9.1 Principles 24

1.9.2 Beer-Lambert law 24

1.10 Scope of project 25

2 MATERIALS AND METHODS 25

2.1 Materials 25

2.2 Catalyst preparation 26

2.3 Catalyst characterization 26

2.3.1 N_2 physisorption 26

2.3.2 H_2-TPR 26

2.3.3 TPD 27

2.3.4 SEM 27

2.3.5 TEM 27

2.4 Catalyst reduction 28

2.5 Lipid extraction using supercritical hexane 28

2.6 Hydrodeoxygenation experiment 29

2.6.1 Semi-batch and batch operations 29

2.6.2 Reactor setup 30

2.7 Analysis 30

2.7.1 Analysis of the liquid phase 30

2.7.2 Analysis of extracted lipids 32

2.7.3 Chlorophylls and carotenoids measurements 35

2.7.4 Thermogravimetric analysis 35

2.7.5 Scanning electron microscopy analysis and EDXA-analysis 35

2.7.6 Fourier transform infrared spectroscopy (FTIR) 35

2.7.7 Organic elemental analysis 36

3 RESULTS AND DISCUSSIONS 36

3.1 Validation of the GC method 36

3.2 Catalyst characterization 36

3.3 Lipid extraction 39

3.3.1 Effect of the extraction time using supercritical hexane as a solvent 39

3.3.2 Effect of stirring speed 41

3.3.3 Characterization of lipid sample produced via supercritical hexane extraction 44

3.4 Hydrodeoxygenation of lipids 53

4 CONCLUSIONS 56

REFERENCES 57

APPENDICES 62

LIST OF ABBREVIATIONS

ASTM	American Society for Testing and Materials
BET	Brunauer-Emmett-Teller
BJH	Barrer-Joiyner-Halenda
BSFTA	N,O-Bis(trimethylsilyl)trifluoroacetamide
DO	Deoxygenation
EDS	Energy-dispersive spectrometer
EDXA	Energy dispersive X-ray analysis
FAME	Fatty acid methyl esters
FFA	Free fatty acids
FID	Flame ionization detector
GC	Gas chromatography
HCH-2-300	Lipids extracted with supercritical hexane at 300 rpm for 2 h
HDO	Hydrodeoxygenation
MDTG	Mono, di and tri-glycerides
MTBE	Methyl tert-butyl ether
OEA	Organic elemental analysis
OPEC	Organization of the Petroleum Exporting Countries
PTFE	Polytetrafluoroethylene
RF	Response factor
SE	Secondary electron
SEC	Size exclusion chromatography
SEM	Scanning electron microscopy
TCD	Thermal conductivity detector
TEM	Transmission electron microscopy
TGA	Thermogravimetric analysis
TMCS	Trimethylchlorosilane

TP	Temperature programmed
TPD	Temperature programmed desorption
TPO	Temperature programmed oxidation
TPR	Temperature programmed reduction
TPRS	Temperature programmed reaction spectroscopy
TPS	Temperature programmed sulfidation

1 INTRODUCTION

In recent years, renewable fuel used for transportation has attracted a huge attention as an alternative and environmentally friendly fuel. There are several reasons for this trend such as a rapid demand in fossil fuels associated with a decrease in reservoirs, unpredictable pricing trends and environmental concerns.

According to the report 'World Oil Outlook' of Organization of the Petroleum Exporting Countries (OPEC) in 2015, diesel/gasoil constitutes the majority of fuel global demand of 29.7% and 32.0% in 2014 and 2040, respectively. In addition, diesel/gasoil is projected to have the fastest growth of 2.3% in 2040, as illustrated in Figure 1. Noticeably, fuel used in the road transport sector accounts almost 60% of the total diesel/gasoil demand. With this in mind, a number of biofuels production processes derived from biomass has recently sparked the interest of academia and industry. Among other biomass resources, fatty acids have proven their potential due to local availability and high heating value in producing biofuels. There are several pathways that have used fatty acids as a feedstock to produce biofuels in laboratory scale as well as in industrial scale.

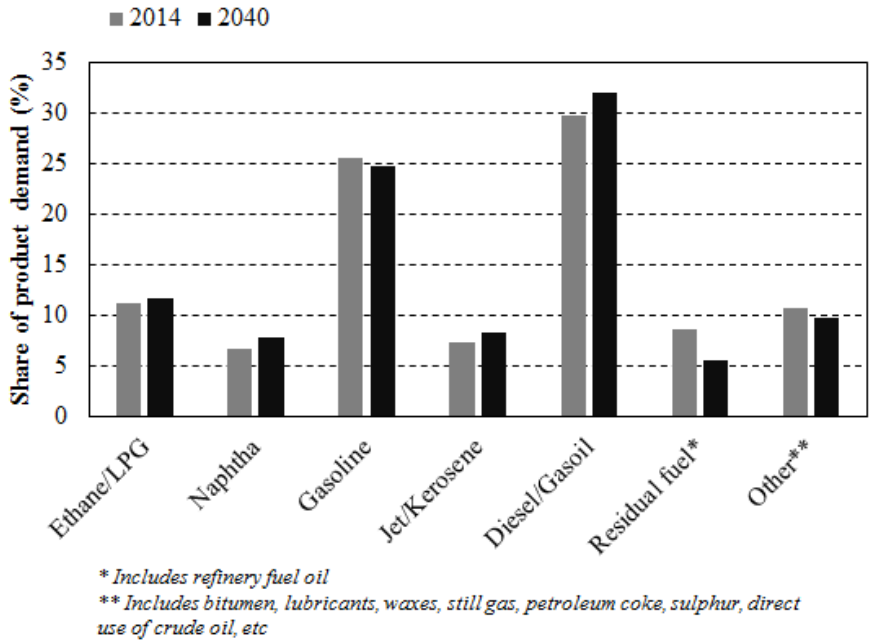

Figure 1. Global fuel product demand from 2014 to 2040

The first generation of biorefinery concept involving biofuel production based on vegetable oils, sugar cane and animal fats has been intensively studied. However, it competes with food production. The second generation of biofuel production using non-edible resources

such as waste vegetable oils and agricultural wastes has also been investigated. This is, however, still limited caused by scant availability of feedstock (Trivedi et al., 2015).

Fortunately, new alternative-algae have been identified as the third generation feedstock for biofuel production due to their oil rich content. *Chlorella* algae are a main feedstock in the present study for green diesel production.

1.1 Feedstock

Algae have recently been identified as attractive feedstocks. First, they could adapt with various living environment such as sea water or wastewater. More importantly, algae could also remove carbon dioxide from the atmosphere via carbon fixation in photosynthesis (Trivedi et al., 2015). This could help algal biomass based fuel to be advantageous by excluding emitted CO_2 known as neutral carbon (Searchinger et al., 2009).

The diversity of feedstock in algae containing protein, carbohydrates and lipids offers many opportunities for refined chemical products and biofuels. For example, proteins mainly contain amino acid, which could be utilized for amino alcohol production, whereas carbohydrates and lipids are the feedstocks for bioethanol or hydrogen and biodiesel or diesel production, respectively (Trivedi et al., 2015). Table 1 presents the composition of different algae.

Table 1. General composition of different algae (wt%) (Trivedi et al., 2015).

Algae	Protein	Carbohydrates	Lipids
Anabaena cylindrica	43–56	25-30	4-7
Aphanizomenon flos-aquae	62	23	3
Arthrospira maxima	60-71	13-16	6-7
Chlamydomonas rheinhardii	48	17	21
Chlorella vulgaris	51-58	12-17	14-22
Chlorella pyrenoidosa	57	26	2
Dunaliella bioculata	49	4	8
Dunaliella salina	57	32	6
Euglena gracilis	39-61	14-18	14-20
Porphyridium cruentum	28-39	40-57	9-14
Prymnesium parvum	28-45	25-33	22-38
Scenedesmus dimorphus	8-18	21-52	16-40
Scenedesmus obliquus	50-56	10-17	12-14
Scenedesmus quadricauda	47	-	1.9
Spirogyra sp.	6-20	33-64	11-21
Spirulina maxima	60-71	13-16	6-7
Spirulina platensis	46-63	8-14	4-9
Synechococcus sp.	63	15	11
Tetraselmis maculate	52	15	3

In the present study, *Chlorella* algae was used as the main feedstock for lipids extraction. The *Chlorella* algae powder was purchased from Luontaistukku, Finland. The composition of *Chlorella* is shown in Table 2 according to manufacturer information. It contains over 60 wt% protein and 12 wt% lipids.

Table 2. Composition of *Chlorella* algae

Components	**Mass (g) in 100 g**
Protein	66
Carbohydrate	23
Lipids	12
Fiber	11
Chlorophyll	3.3

1.2 Biorefinery

Biorefinery concept refers to a sustainable biomass processing in which energy, biofuels and high valuable products are obtained via biomass transformation. Particularly, algal biorefinery has been considered as a promising concept because of its potential to produce multiple products by availing of different biomass components. In addition to economic benefits, biorefinery based on algae could deal with several environmental and sustainable issues such as greenhouse gas emission, fossil fuel dependence, land use for fuel production (Trivedi et al., 2015). The latter issue is really important when the land used for fuel production can be also utilized for food production.

In this study, the aim was to produce green diesel from lipids originated from *Chlorella* algae.

1.3 Cell disruption and lipid extraction

Hitherto, numerous techniques for lipid extraction have been developed, especially industrial-scale application have been attractive due to the growth of algae-based biofuel industry. However, algal lipid extraction at commercial level is still at its infancy (Theegala, 2015, p.420). One of the most common difficulties regarding the lipid extraction is to break

cell walls of algae so called as cell disruption. Various methods have been employed for cell disruption such as microwaves, sonification and bead-beating, high pressure homogenization, heat disruption, etc (Theegala, 2015, pp.423–424).

Traditionally, lipid extraction is widely carried out via Bligh and Dyer's method (Bligh and Dyer, 1959). However, the involvement of toxic solvents such as chloroform and methanol is the main barrier for their large scale application concerning health risks and environmental issues. Although hexane is less efficient for lipid extraction from algae than the above mentioned solvents (Lee, Yoon and Oh, 1998), minimal non-lipid contaminants and higher selectivity towards neutral lipids fraction could be achieved by hexane (Shin et al., 2014). In order to penetrate the thick cell wall of algae, supercritical fluids of carbon dioxide have been studied for lipid extraction (Mariod, Matthäus and Ismail, 2011; Mouahid, Crampon, Toudji and Badens, 2013; Taher et al., 2014). A supercritical state of hexane might be advantageous for lipid extraction in industrial scale due to its higher selectivity for neutral lipids and ease of solvent recovery. However, lipid extraction with supercritical hexane is still limited. In a previous study, lipids were extracted from *Scenedesmus* sp. with supercritical hexane for biodiesel production (Shin et al., 2014), in which fatty acid methyl esters (FAME) were considered as a comparative parameters.

Lipids contained in algae can be classified into neutral or non-polar lipids and polar lipids. The former comprises of acylglycerols (mono, di and tri-glycerides-MDTG), free fatty acids (FFA) and pigments (chlorophyll and carotenes). The latter consists of phospholipids and glycolipids (Shin et al., 2014; Li et al., 2014). Depending on the solvent polarity used in algal lipid extraction methods, the corresponding lipids would be separated.

1.4 Biodiesel production

Nowadays, biodiesel is a widely used definition of diesel fuel composed of fatty acid methyl esters originating from renewable feedstock. Transesterification has been considered as a popular pathway for biodiesel, which constitutes alkyl esters of long chain fatty acids. Feedstock or raw material for biodiesel production is diverse including vegetable oils or animal fats which mainly contain triglycerides. Scheme 1 shows the general transesterification reaction in which triglycerides are the feedstock.

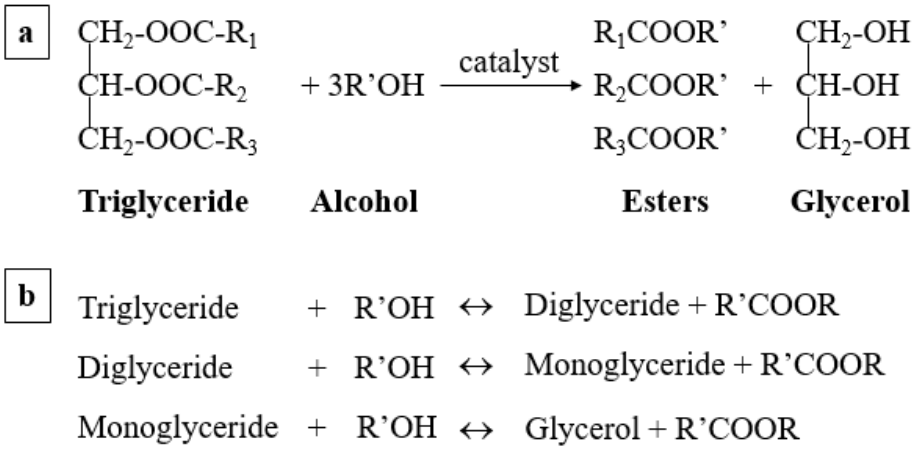

Scheme 1. Transesterification of (a) triglyceride and (b) partial reactions in transesterification process (adapted from (Enweremadu and Mbarawa, 2009)).

Biodiesel has been attractive for both business and academia for decades due to renewability and environmental friendliness. It has been widely used, since it can be blended with conventional diesel or used directly. Nevertheless, inherent drawbacks of biodiesel, mainly cold flow properties and chemical instability due to fatty acid esters and engine compatibility issues are the major barriers to its commercialization (Santillan-Jimenez and Crocker, 2012).

1.5 Green diesel production

In order to overcome the inherent drawbacks of biodiesel, while utilizing the renewable feedstock for biofuel production, a relatively new pathway has been studied (Santillan-Jimenez and Crocker, 2012). Hydrodeoxygenation (HDO) is a technology which can remove oxygen in form of water (H_2O) from biomass, particularly, from triglyceride and fatty acids to produce hydrocarbons. HDO reactions are illustrated in Scheme 2. The formed hydrocarbons can be used as a diesel fuel for current diesel engine without any modification.

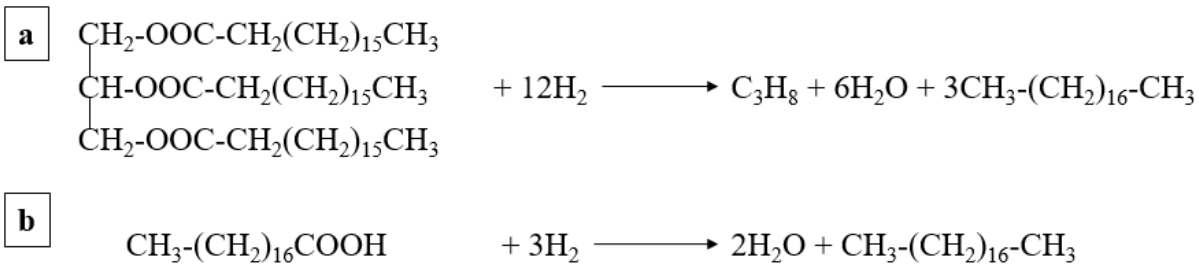

Scheme 2. Hydrodeoxygenation of (a) tristearin as a model triglyceride and (b) stearic acid as a model fatty acid (adapted from (Santillan-Jimenez and Crocker, 2012)).

There are several commercial processes that produce hydrocarbon fuels from vegetable oil or animal fats. In 2007, Neste Oil Oy has commercialized NExBTL renewable diesel process (Santillan-Jimenez and Crocker, 2012). Recently, UPM in Lappeenranta, Finland has also introduced their renewable diesel as UPM BioVerno using crude tall oil as feedstock.

The green diesel produced by hydrodeoxygenation has shown its potential in order to be commercialized due to compatibility with current diesel engine. Compared to biodiesel, it is however, produced much less.

Deoxygenation including decarboxylation and decarbonylation has been studied in addition to HDO for green diesel production. Deoxygenation has been attractive due to lower consumption of hydrogen. Scheme 3 shows deoxygenation of stearic acid. However, it is noted that insufficient hydrogen leads to higher formation of aromatic compounds which play a key role in catalyst deactivation (Mäki-Arvela et al., 2011; Santillan-Jimenez and Crocker, 2012).

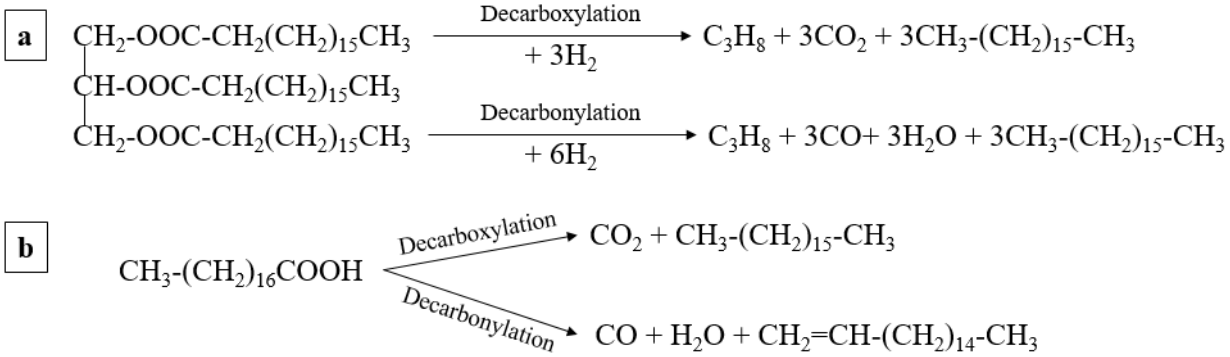

Scheme 3. Deoxygenation of (a) tristearin as a model triglyceride and (b) stearic acid as a model fatty acid (b) (adapted from (Santillan-Jimenez and Crocker, 2012)).

1.6 Catalysts

Many reactions such as catalytic cracking, hydrocracking, alkylation, isomerization, esterification, oligomerization and hydrolysis could be carried out by acid-catalyzed processes (Sheldon, Arends and Hanefeld, 2007, p.49). On the one hand, according to the definition of Brønsted and Lowry, acids are proton donors. On the other hand, Lewis acids are defined as electron-pair acceptors.

1.6.1 Zeolite as catalysts and supports

Zeolites that are known as molecular sieves with formulae described as $Na_x[AlO_2)_x(SiO_2)_y][H_2O]_y$. A tetrahedral structure of zeolites has each atom of silicon and aluminum surrounded by oxygen atoms shown in Figure 2 (Rao, 2007).

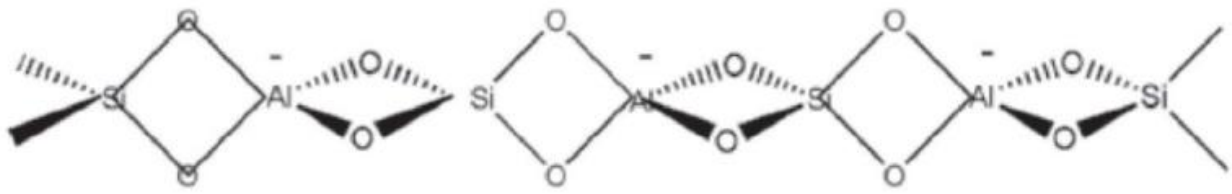

Figure 2. The structure of zeolite (Rao, 2007).

In the early 1950s-the beginning of the discovery of synthetic zeolites, they were applied commercially for commodity fuels and petrochemicals production. Application of zeolites in petroleum industry has brought many environmental and economic benefits including a steady increase of the amount of clean fuel product per barrel of oil. This resulted in reducing emissions of CO_2, NO_x, SO_x and particulates and increasing energy efficiency. The efficiency of zeolites is reasonable. 3000-500000 weight units of fuel or petrochemical products can be produced by each weight units of zeolites before its life span ends (Brown, 2010, pp.2–4)

Zeolites have been used for acid-catalyzed reactions due to their acidity. The acid strength of zeolite is based on the Si/Al ratio. The lower the Si/Al ratio is (increase of aluminum content), the stronger the acidity of zeolite is (Simon-Masseron et al., 2007; Rakić and Damjanović, 2013). More importantly, molecular sized cavities contained in a regular structure makes zeolites unique as shape selective for a wide range of organic transformations (Sheldon, Arends and Hanefeld, 2007, pp.53–54).

Zeolite studied in this work is a synthetic zeolite Y which has the faujasite framework as illustrated in Figure 3.

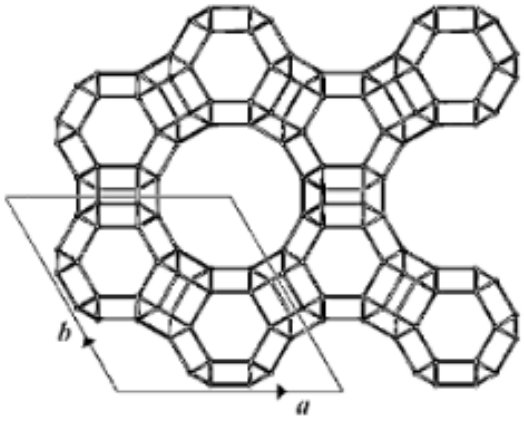

Figure 3. Faujasite framework type of zeolite Y (Sheldon, Arends and Hanefeld, 2007, p.55).

1.6.2 Metal as active site for (hydro)deoxygenation reaction

Catalytic deoxygenation of fatty acids has been reported in the pioneering work of our laboratory (Kubičková et al., 2005). The activities of supported metal catalysts increased in the order of Pd>Pt>Ni>Rh>Ru>Os for DO of stearic acid under constant pressure and temperature of 6 bar and 300 °C, respectively (Snåre et al., 2006). Therefore, Pd has been extensively studied in terms of productivity and selectivity for DO reaction. In 2011, Mäki-Arvela et al. investigated tall oil fatty acids as a feedstock for deoxygenation (DO without hydrogen atmosphere) of fatty acids with 1% Pd/C used as the catalyst. The result showed that the highest selectivity of 82% to n-heptadecane and n-heptadecene was achieved at 300-325 °C when the lowest initial rate TOFA concentration was used. It was also reported that the presence of hydrogen increased selectivity towards the desired hydrocarbon (Mäki-Arvela et al., 2011). In another study, Pd supported on SBA mesoporous 5% Pd/Al-SBA-15 with different acidic strength (Si/Al molar ratio) was applied. It was concluded that high acidity of the catalyst was not favorable for HDO of sunflower oil at high temperature (Duan et al., 2012).

In recent years, several studies were performed in HDO by thoroughly investigating influences of different catalysts. In addition to Pd and Pt, other noble metals were also employed such as Ru, Ir, Os and Rh. However, the results were not so promising. Nickel (Ni), a non-noble metal, however has shown its great potential for deoxygenation in

industrial application. The price of Ni is 1000 and 2500 times lower than Pd and Pt, respectively (Santillan-Jimenez and Crocker, 2012).

Kumar et al. carried out the investigation of Ni on different types of supports including SiO_2, γ-Al_2O_3 and HZSM-5 for HDO of stearic acid in the temperature of 260-290 °C (Kumar, Yenumala, Maity and Shee, 2014). The highest selectivity toward n-heptadecane of 80% was achieved with Ni supported on γ-Al_2O_3 after 4 h. It was also reported that higher conversion was achieved by increasing reaction time, nickel loading on γ-Al_2O_3, temperature and catalyst loading. In other finding in which microalga oil extracted from *Nannochloropsis* salina was performed continuous HDO over several catalysts (Zhou and Lawal, 2016), $NiMo/Al_2O_3$ was observed to have 13.8% lower hydrocarbon yield compared to 1% Pt/Al_2O_3. The reaction conditions for $NiMo/Al_2O_3$ is at 360 °C, 35 bar, 1000 SmL/mL gas/oil ratio and 1s residence time, whereas HDO over 1% Pt/Al_2O_3 was performed at 310 °C, 35 bar, 1000 SmL/mL gas/oil ration and 1.5 residence time.

1.7 Characterization techniques

In order to explain the productivity of HDO reaction, it is essential to understand the characteristics of the catalyst which is one of the key factors in HDO reaction. Several characterization techniques were used to investigate the structural and textural properties of the catalysts.

1.7.1 N_2 physisorption

Nitrogen adsorption at the boiling point of -196 °C (77 K) is the most widely used method for determination of specific surface area and porous catalyst texture. Obtained plural data from N_2 physisorption provide information in terms of specific surface area, pore volume and size distribution. The Brunauer-Emmett-Teller (BET) remains the most common method for calculation of the surface area described by following equation. It is noted that BET method is only accordance with mesoporous structure (Leofanti, Padovan, Tozzola and Venturelli, 1998; Sing, 2001). The specific surface area is calculated as

$$A_s = (\frac{V_m}{22414})N_a\sigma \qquad (1)$$

Where

V_m: monolayer volume of the adsorbate (cm^3/g)

A_s: the surface area

N_a: Avogadro number

σ: accepted as 0.162 mm^2 in case of nitrogen at -196 °C.

Monolayer volume-V_m could be estimated by two parameters BET equation (Leofanti et al., 1998):

$$V_{ads} = V_m \frac{cp/p_s}{(1-p/p_s)(1+(c-1)p/p_s)} \quad (2)$$

Where

V_{ads}: adsorbed volume of gas (cm^3/g)

p/p_s: relative pressure

c: parameter related to heat of adsorption and liquefaction.

IUPAC has classified the isotherms for the amount of adsorbed gas as a function of the equilibrium pressure in the way shown in Figure 4. However, only four adsorption isotherms are usually observed in catalyst characterization including type I, II, IV and VI (Leofanti et al., 1998). Type I and IV are typical for zeolites or microporous solids and mesoporous solids, respectively (Leofanti et al., 1998; Llewellyn, Bloch and Bourrelly, 2012, p.863).

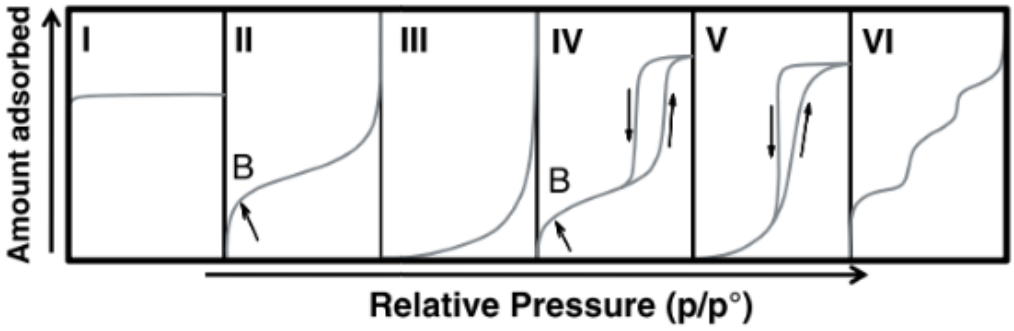

Figure 4. Six isotherm classified by IUPAC (Llewellyn, Bloch and Bourrelly, 2012, p.863).

In addition to specific surface area, N_2 physisorption also provides determination of pore size distribution. One of the most widely used methods, which is recommended by ASTM standard D4641/87 and applied in various commercial instruments is the Barrer-Joyner-Halenda (BJH) method (Barrett, Joyner and Halenda, 1951). BJH method mainly applied for calculations of mesopores uses the Kelvin model to define r_c- the Kelvin radius described below (Leofanti et al., 1998)

$$\ln(p/p_s) = -\frac{2\gamma\omega_m cos\theta}{RTr_c} \quad (3)$$

Where

r_c- Kelvin radius (m)

γ: the surface tension of liquid condensate (N/m)

ω_m: molar volume (cm^3/mol)

θ: the contact angle

R: gas constant (8.314 J/K.mol)

T: temperature (K)

Statistical thickness-t, which is necessary to get the real pore radius could be obtained from the standard isotherm defined by the following equation

$$t = 3.54\left(\frac{5}{\ln(p/p_s)}\right)^{1/3} \quad (4)$$

Finally, pore radius r_p is obtained by the equation

$$r_p = r_c + t \quad (5)$$

1.7.2 Temperature programmed techniques

Temperature programmed (TP) techniques involve monitoring chemical reactions while temperature is increasing linearly with time. TP techniques are divided into different classes including temperature programmed reduction (TPR), temperature programmed oxidation (TPO), temperature programmed sulfidation (TPS), temperature programmed desorption (TPD) and temperature programmed reaction spectroscopy (TPRS) (Niemantsverdriet, 2007b, p.11). In the current work, TPR and TPD which are mainly used for catalyst characterization will be discussed.

1.7.2.1 Temperature program reduction

Reduction is a crucial step in catalyst preparation as if it is not performed correctly or sufficiently, the catalyst may sinter or an optimum state of the metal need in catalysts could not be reached. The reduction of a metal oxide MO_n by H_2 is described by the following equation (Niemantsverdriet, 2007b, p.13)

$$MO_n + nH_2 \rightarrow M + nH_2O \quad (6)$$

Temperature needed for complete catalyst reduction could be determined from TPR (Niemantsverdriet, 2007b, p.18). Besides, TPR profiles provide the information regarding the reduction state of the catalyst analyzed. The area under TPR curve represents the consumption of hydrogen for the catalyst reduction which is commonly presented as moles of hydrogen consumed per mole of metal atoms (Rakić and Damjanović, 2013, p.144).

1.7.2.2 Temperature programmed desorption of NH_3

TPD of NH_3 is used in catalyst characterization to determine the number, type and strength of acid sites on the surface. In this case, NH_3 acts as an adsorbate on the catalyst acting as an adsorbent. Contrary to TPR in which hydrogen consumption is monitored with time, TPD relates the gas desorbed gas with the temperature increased. It is considered that desorption at lower temperature refers to weaker acid sites and vice versa. The area under the TPD curve is proportional to the amount of desorbed NH_3 as a function of temperature (Rakić and Damjanović, 2013, p.142).

1.7.3 Electron microscopy

In order to study thoroughly the catalyst structure at the atomic scale, electron microscopy is widely used providing necessary resolution. Two main methods are usually employed including scanning and transmission electron microscopy.

1.7.3.1 Scanning electron microscopy and X-ray microanalysis

Scanning electron microscopy (SEM) provides observation and characterization of heterogeneous organic and inorganic materials in the scale from nanometer (nm) to micrometer (μm). The major advantage of SEM is that high resolution of observation of bulk objects could be obtained in the range of 1-5 nm (Goldstein et al., 2003, pp.1–2). There are two types of electrons including secondary electrons (SE) and backscattered electrons (BSE) emitted depending on the position of the primary beam. The former originates from the surface layers of a sample which are characterized by low energies (≈ 5-50 eV). The latter emitted from a deeper layer provides the composition of a sample due to highly reflective heavy elements appearing brighter in the image (Niemantsverdriet, 2007a, p.184). SEM is nowadays equipped with energy-dispersive spectrometer (EDS) which is able to measure X-rays emitted from the elements. EDS facilities could offer a rapid detection of all elements above atomic number 4. EDS X-ray is capable of carrying out accurately quantitative analysis (Goldstein et al., 2003, pp.11–12). In case higher resolution is required,

transmission electron microscopy is more favorable than SEM (Niemantsverdriet, 2007a, p.185).

1.7.3.2 Transmission electron microscopy

Transmission electron microscopy (TEM) operates at higher energy of electrons in the range of 100-200 keV. In addition, high vacuum environment, for example, 10^{-6} mbar is employed to avoid collisions of the electron beam with molecules in the gas phase (Rochow and Tucker, 1994, p.294; Niemantsverdriet, 2007a, p.183). The major advantage of TEM is that higher resolution, for example, 0.3 nm, is achievable (Niemantsverdriet, 2007a, p.183). It is important to consider that increasing the contrast may lead to a loss of resolution (Cowley, 2005, p.462).

1.8 Analysis of liquid phase

The liquid phase analysis is mainly performed with gas chromatography equipped with flame ionization detector (GC-FID) to determine the components. Internal standard method is used to quantity the amount of each component in samples.

1.8.1 Gas chromatography

Gas chromatography (GC) was introduced for the first time by James and Martin in 1952. The identification of components in a mixture is made by a time separation of each analyte. The basic principle of gas chromatography is that sample is volatized in a heated inlet port called injector, thereafter, each component in a mixture will be separated in a special column and detected by a detector. In GC, the carrier gas such as hydrogen or helium plays an important role to transfer the sample from the injector through the column and into the detector. The column in GC is composed of a coating of a stationary phase. Components in a sample are separated based on their distribution between the carrier gas acted as a mobile phase and the stationary phase. The identification of each component is based on its spending time in a column called retention time. The lower is the staying time of an analyte in the column, the faster the elution will be. Only volatile substance are suitable to be used in GC (Kitson, Larsen and McEwen, 1996, p.3).

1.8.2 Gas chromatography/flame ionization detector (GC-FID)

A component in the effluent comes into the flame ionization detector (FID) and passes through a hydrogen/air flame. The flame formed contains ions and electrons causing a

current to flow in the gap between two electrodes in the detector. The current to flow will be amplified to produce a signal (Kitson, Larsen and McEwen, 1996, p.7).

1.8.3 Gas chromatography/mass spectrometry (GC-MS)

Mass spectrometry was developed by J.J. Thomson in 1913 who is called as "father of mass spectrometry". Mass spectrometry measures the mass-to-charge ration (m/z) of gas phase ions and quantities the amount of each ionic species. The measurement is calibrated against ions of known m/z. Gas phase ions are separated by the interaction of magnetic or electrical fields on charged particles under a low pressure environment (Kitson, Larsen and McEwen, 1996, p.9).

1.8.4 Principle of internal standard method

The principle of the internal method is based on a response factor (RF) of each component in a mixture. It is especially useful method when the group definition is required. The response factor of each component is determined with known concentrations of the internal standard and a component. The calculation of the response factor is described below

$$RF_i = \frac{S_{IS}}{S_i} \times \frac{n_i}{n_{IS}} \qquad (7)$$

Where

RF_i: response factor of component i

S_{IS}: peak area of the internal standard

S_i: peak area of component i

n_{IS}: mass of the internal standard in the volume of standard sample injected into chromatograph

n_i: mass of component i in the volume of standard sample injected into chromatograph

The calculated RF for each analyte will be used for its quantification in a mixture with unknown concentration. The calculation of each analyte is done by the following equation

$$n_i = RF_i \times \frac{n_{IS}}{S_{IS}} \times S_i \qquad (8)$$

Where:

n_i: mass of component I in the volume of sample injected into chromatograph

RF_i: response factor of component i calculated by equation (7)

S_i: peak area of component i

n_{IS}: mass of the internal standard in the volume of sample injected into chromatograph

S_{IS}: peak area of the internal standard

1.8.5 Validation of the method

In order to verify that the concentration of a certain component in the sample is within the detection limit, the linearity between the peak area and the concentration should be studied. Heptadecene, palmitic and stearic acids were chosen for investigation in a range of concentration from 1 to 10 mg/mL, while the concentration of the internal standard was fixed to 10 mg/mL. The internal standard-eicosane was separately studied as a blank sample with the similar concentration range of 1-10 mg/mL.

1.9 UV-Vis spectroscopy

1.9.1 Principles

Many molecules absorb ultraviolet or visible light. The absorbance of a solution increases as attenuation of the beam increases. Absorbance is directly proportional to the path length, b, and the concentration, c, of the absorbing species. Beer's Law states that A = εcl, where ε is a constant of proportionality, called the absorptivity and c is the concentration of substance, l is the width of a layer through which the light passes.

Different molecules absorb radiation of different wavelengths. An absorption spectrum will show a number of absorption bands corresponding to the structural groups within a molecule

1.9.2 Beer-Lambert law

Beer-Lambert law is commonly used for transformation of absorbance into concentration. Figure 5 shows the adsorption of light beam which passes through the cuvette containing the substance. Beer-Lambert law is usually presented in the following form.

$$I = I_0 10^{-\varepsilon c l} \qquad (9)$$

Where

I_0: the intensity of the incident light

I: intensity of the transmitted light through the cuvette

ε: the adsorption coefficient which is specific for substance (constant value)

c: the concentration of substance

l: the width of layer, typically cuvette through which the light passes.

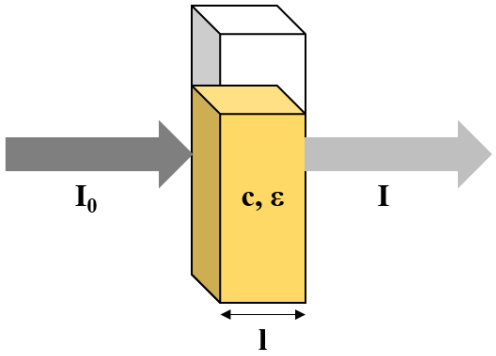

Figure 5. Adsorption of light beam passing through cuvette

Lambert-Beer law can be shown in the following way after being taken logarithm

$$A = \lg\left(\frac{I_0}{I}\right) = \varepsilon c l \qquad (10)$$

Where

A: absorbance of the substance.

Therefore, it is clear that the concentration of the solution is directly proportional to its absorbance.

1.10 Scope of project

To our best knowledge, there are no previous reports concerning direct hydrodeoxygenation of lipids extracted from algae. The aim of this work is to provide a comprehensive study and to demonstrate for the first time hydrodeoxygenation of lipids extracted from *Chlorella* algae. The project has the following objectives:

- To determine optimum conditions for lipid extraction from *Chlorella* using supercritical hexane.
- To provide a comprehensive study of the lipids extracted from algae by supercritical hexane
- To demonstrate hydrodeoxygenation of the extracted lipids.

2 MATERIALS AND METHODS

2.1 Materials

Chlorella algae purchased from Luontaistukku, Finland were used without any pre-treatment. According to the manufacturer, *Chlorella* algae contain over 60% protein and

12% lipids. The catalysts used for HDO experiments have been prepared and characterized previously in our lab (Hachemi et al., 2016). Other chemicals used in this work are analytically graded.

2.2 Catalyst preparation

Two Ni catalysts 5 wt% Ni/H-Y-80 and 5 wt% Ni/SiO_2 were prepared and tested in this work. The Ni on H-Y-80 catalyst was prepared by a wet impregnation-evaporation method. The synthesis of 5 wt% Ni/H-Y-80 was conducted by the following procedure. Preliminary, the commerical zeolite H-Y-80 (Zeolyst International, SiO_2/Al_2O_3 ratio of 80) was calcined at 400 °C for 4 hours then sieved with a 63 µm sieve to obtain identical particle size. Simultaneously, nickel(II) nitrate hexahydrate solution was prepared with ionized water in a round bottom flask; pH of solution was 6.1. The calcined H-Y-80 was introduced into the nickel(II) solution, giving pH of 3.2. The mixture was rotated for 24 hours in oil bath at 60 °C. The impregnation of Ni on zeolite was made by evaporating water. Finally, the catalyst was dried overnight at 100 °C, then calcined at 400 °C for 3 hours. The calcined catalyst was stored and must be reduced (procedure described in Section 2.4) before the HDO experiment. In a similar manner, 5 wt% Ni/SiO_2 (Silica Gel 60, Merck) was prepared by introducing SiO_2 into nickel(II) solution.

2.3 Catalyst characterization

2.3.1 N_2 physisorption

Surface area and pore volume of the catalysts were determined with N_2 physisorption instrument Sorptomter 1900 from Carlo Erba Instrument. Nitrogen liquid at -196 °C (77 K) was used. Samples were outgassed at 150 °C for 3 hours prior the measurement. The specific surface area was calculated based on BET isotherm, whereas BJH model was used to determine pore size distribution.

2.3.2 H_2-TPR

Temperature programed reduction of the catalysts was conducted with Autochem 2910 apparatus (Micromeritics). Prior to measurements, the samples were dried overnight at 100 °C in order to eliminate moisture. In a typical experiment, 100 mg of sample was added into U-shaped quartz tube. The reduction was performed from room temperature to 650 °C at a constant heating rate of 5 °C and a volumetric flow rate of hydrogen of 50 mL/min. The

desorbed gases from the catalyst surface were detected by a thermal conductivity detector (TCD).

2.3.3 TPD

Temperature programed desorption was performed with the same instrument used in TPR study. Preliminary, the samples were kept overnight at 100 °C to eliminate water. Thereafter, the samples were heated up to 300 °C with the heating rate of 30 °C/min in He, maintained in 10 min. The catalysts were then cooled down and exposed with 5 vol% NH_3 in He and 100% CO_2 in order to determine acid and base strength, respectively. Desorption of gases was performed by raising temperature up to 900 °C with a heating rate of 20 °C/min; thereafter the temperature was hold at 900 °C for 30 min. The amount of desorbed gases was quantified by TCD.

2.3.4 SEM

SEM measurements were carried out by LEO Gemini 1530 with a Thermo Scientific UltraDry Silicon Drift Detector for characterization of chemical composition of the catalyst and morphology on the surface. SE (secondary electron) and backscattered electron (BSE) emitted were detected by corresponding detectors including SE and BSE detectors, respectively. Prior to measurements, the samples were made to be conductive by coating them with carbon.

2.3.5 TEM

High resolution TEM images were made from raw and spent algae. Raw algae and spent algae samples were treated with 5 wt.% KOH in ethanol. The treated algae samples were then fixed with the 5% glutaraldehyde solution in 0.16 mol/L s-collidine buffer and then followed by 2% OsO_4 containing 3% potassium ferrocyanide in 2 h. The samples were dehydrated with different ethanol concentrations of 70%, 96% and 2 times at 100% and embedded in 45359 Fluka Epoxy Embedding Medium kit. A 70 nm thickness of samples were made with an ultramicrotome and stained with 1% uranyl acetate and 0.3% lead citrate. Those thin sections were scanned by a JEOL JEM-1400 Plus TEM operated at 80 kV acceleration voltage integrated with Quemesa 11 MPix bottom mounted digital camera providing a resolution of 0.38 nm.

The distribution of nickel particle size was obtained from TEM image by using a JEOL JEM-1400 Plus TEM operated at 120 kV. Nickel catalyst sample was suspended in ethanol at room temperature by ultrasound, thereafter coated on a grid covered with a carbon film

2.4 Catalyst reduction

The pre-dried catalyst, 0.25 g, was added to quartz-tube and placed into furnace. Quartz-tube was initially flushed with an Ar flow of 20 mL/min for 3 min and thereafter with H_2 at 20 mL/min for 3 min. The furnace was sealed with quartz-wool and temperature program used for catalyst reduction was obtained from TPR which is specific for each type of catalyst. In particular, for 5 wt% Ni/H-Y-80, the temperature was raised from 25 °C to 350 °C in 80 min and kept constant for 120 min. Thereafter, argon flow was switched on; quartz-wool was removed. The reactor was cooled down. Before disconnection of the quartz-tube, 20 mL dodecane was poured into the tube to cover the catalyst, thus avoiding oxidation of the catalyst. The mixture of the catalyst and dodecane was stored overnight before usage. The reduced catalyst was transferred into the reactor; 20 mL dodecane was used to rinse the quartz-tube.

2.5 Lipid extraction using supercritical hexane

Supercritical region is obtained when temperature and pressure of fluids are raised above their critical values. In the present work, hexane was used as a solvent to extract non-polar lipids due to the fact that hexane is less toxic than chloroform. The supercritical state of hexane is achieved when temperature and pressure are raised over its critical point (234.6 °C and 30.3 bar) (Theegala, 2015, p.434).

The supercritical lipid extraction was carried out in the autoclave shown in Figure 7. In a typical experiment, 5 g algae were added into the reactor followed by introduction of 100 mL hexane. Argon was then purged to the reactor to remove air to avoid even a minimal risk of explosion. The reaction mixture was heated to the desired temperature of 235 °C. The pressure was obtained itself by high vapor pressure of hexane of approximately 34 bar at this temperature. Both temperature and pressure were monitored using temperature and pressure controllers. The agitation was set to the desired speed. When extraction was complete, the mixture was cooled to room temperature by using a water cooling coil and depressurized. Algal biomass was separated by filtration. Non-polar lipids were obtained by removal of hexane with a rotavapor. The extracted lipids were weighed gravimetrically and analyzed by a series of analytical methods including TEM, SEC, GC-MS, GC-FID and TGA. Figure 7a

and b present the different steps in supercritical hexane extraction of algal biomass and the reactor setup, respectively.

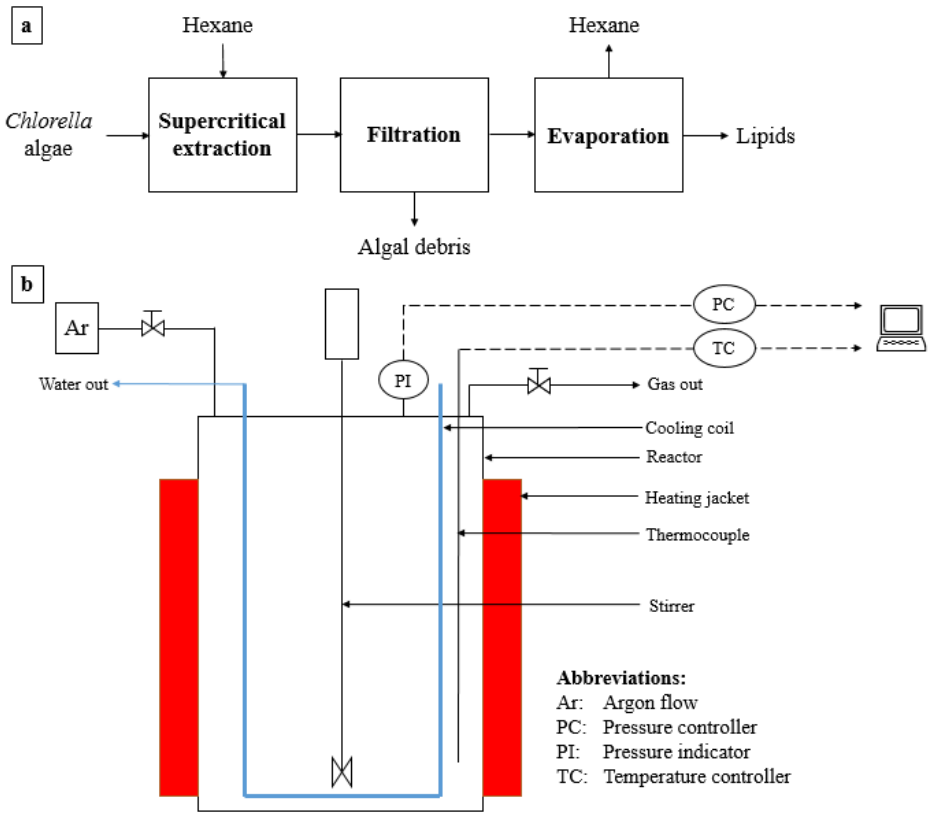

Figure 7. Schematic diagram (a) and schematic picture of the reactor (b) of supercritical lipid extraction of *Chlorella* algae

2.6 Hydrodeoxygenation experiment

2.6.1 Semi-batch and batch operations

Hydrodeoxygenation reaction was carried out in a 300 mL Parr autoclave equipped with a heating jacket. Flow and pressure controllers were employed to control the flow of carrier gas and pressure, respectively. The reaction temperature and pressure were registered and monitored during the reaction. HDO was carried out in an autoclave at 300 °C and under the total pressure 30 bar in H_2. A stirring speed of 1200 rpm was used to overcome the external and internal mass transfer limitation. In semi-batch operation, gaseous phase was continuously fed into the reactor to keep the reaction pressure constant. In batch operation, by contrast, reaction pressure increases slightly as there was no removal of gaseous phase.

2.6.2 Reactor setup

The catalyst was preliminary reduced (procedure was described in Section 2.4) before being added into the reactor. The solvent was added into the bubbling unit in which it was preheated to 100 °C to decrease its viscosity; this could help to avoid solvent losses during the transfer into the reactor. Thereafter, the reactor was thoroughly flushed with argon. The reaction mixture was heated to the desired temperature at 10 °C/min and pressurized with H_2 AGA 99.999% to 30 bar. After reaching the desired temperature, the stirring started (1200 rpm) and reaction time was set to be zero at that time. In a typical experiment, 1 g of reactant and 100 mL dodecane and 0.25 g catalyst were used. The samples were taken at the following intervals: 0, 30, 60 and 360 minutes for kinetic analysis. All collected samples were analyzed by a gas chromatography (procedure described in the next section). Figure 8 shows the semi-batch reactor system.

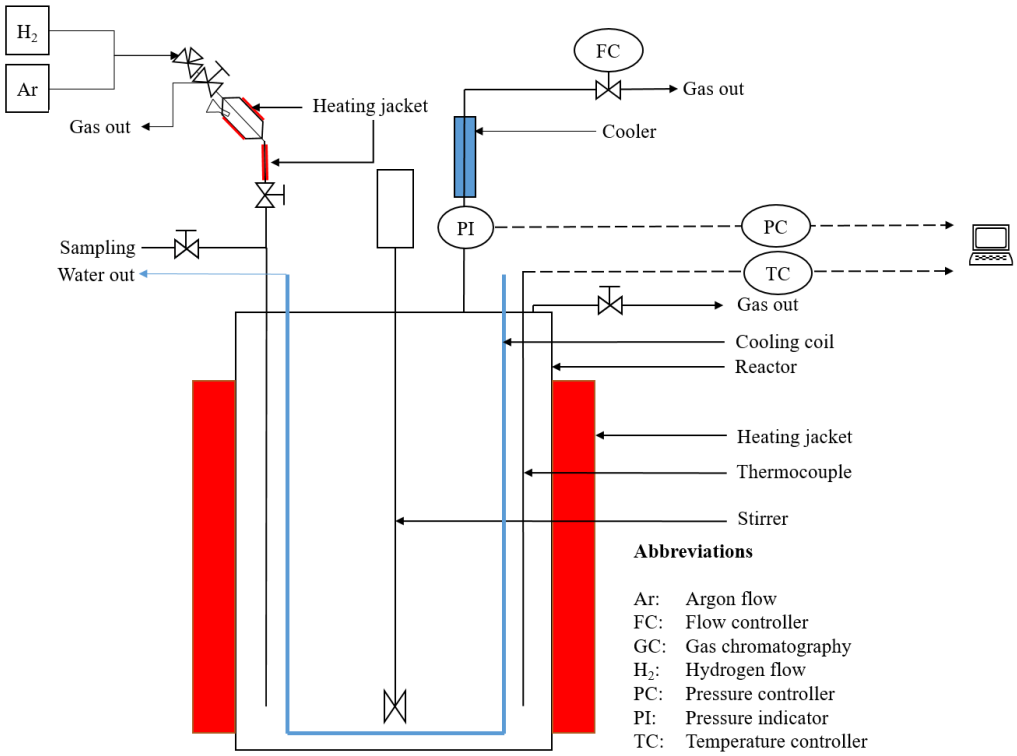

Figure 8. Semi-batch reactor system used in HDO experiment

2.7 Analysis

2.7.1 Analysis of the liquid phase

The components in the liquid phase containing hydrocarbons, FFA and FAME were identified by the comparison of their retention times with those of authentic standards and

quantified by the internal standard method. The sample preparation for analysis is described below.

The samples after being collected in glass vials were stored in the fridge at 4 °C. Thereafter they were silylated by the following procedure: 0.1 mL of a sample was diluted in 1 mL pyridine (Sigma-Aldrich, ≥ 99%). After that 0.1 mL of eicosane (10 mg/mL) (Acros Organics, 99%) was added as an internal standard associated with 0.1 mL of BSFTA (Acros Organics, ≥ 98%) and 0.05 mL of TMCS (Sigma Aldrich, ≥ 98%). The samples were subsequently silylated in an oven at temperature of 70 °C for 60 minutes. Finally, the samples were naturally cooled down before being injected to a gas chromatograph with a flame ionization detector (GC-FID) under the conditions: injection volume of 1 μL, He pressure of 14.5 psi with a flow velocity of 75 mL/min, a capillary column (ZB-5HT Inferno, length of 30 m, internal diameter of 0.32 mm and film thickness of 0.25 μm), oven program from initial temperature of 70 °C to 205 °C at 5 °C/min hold 18 min, and then to 300 °C at 7 °C/min hold 15 min. The signals were recorded by FID.

Since the triglyceride fraction cannot be detected by GC-FID with a long capillary column, it was treated and analyzed by GC-FID equipped with a short column – an Agilent J&W HP-1/SIMDIST column (cut length of 7 m, internal diameter of 0.53 mm and film thickness 0.15 μm). The collected samples were filled by 2 mL of methyl tert-butyl ether (MTBE) containing the following internal standards (0.04 mg/internal standard): heneicosanoic acid (C21:0, Sigma-Aldrich, 99%), betulinol (purified in our lab), cholesteryl heptadecanoate (Sigma-Aldrich, >95%) and 1,3-dipalmitoyl-2-oleoglycerol (Sigma-Aldrich, 99%). Docosanol was concentrated by evaporating MTBE at 40 °C under nitrogen stream. The evaporation was repeated after adding 1 mL of acetone. 150 μL of the silylation reagent mixture including pyridine, BSTFA and TMCS (1:4:1 v/v/v) was added and the final mixture was silylated in oven at 70 °C for 45 minutes. The silylated samples were analyzed by PerkinElmer Clarus 680 Gas Chromatograph equipped with a FID and a short column mentioned above, oven program from the initial temperature of 100 °C hold 0.5 min, and then heating to 340 °C at 12 °C/min and hold 5 min.

The mass fraction of fatty acids or FAME denoted as i was calculated as

$$X[\%] = \frac{c_i^t}{c_i^0} \times 100 \quad (10)$$

Where

c_i^0: the concentration of i at the beginning of reaction (t=0)

c_i^t: the concentration of i at time t

The conversion of i was calculated as

$$C[\%] = \frac{c_i^0 - c_i^t}{c_i^0} \times 100 \quad (11)$$

Where

c_i^0: the concentration of stearic acid at the beginning of the reaction (t=0)

c_i^t: the concentration of stearic acid at time t

The calculation of the yield of C17 hydrocarbon corresponding to stearic acid is presented by following equation

$$S[\%] = \frac{c_{C17}^t}{c_{others}^t} \times 100 \quad (12)$$

Where

c_{others}^0: the concentration of other products

c_{C17}^t: the concentration of C17 hydrocarbon at time t

The calculations of conversion and selectivity shown above are for stearic acid as a feedstock and C17 hydrocarbon as a desired product. In other cases, the calculation for other hydrocarbons corresponding to fatty acids or FAME having similar carbon atoms could be adjusted.

2.7.2 Analysis of extracted lipids

Lipids extracted from *Chlorella* algae by supercritical hexane contain non-polar lipids. In order to identify the optimum conditions for supercritical lipid extraction, the extracted lipids were weighed gravimetrically to obtain the lipid yield which was calculated as shown below

$$Y[\%] = \frac{OL}{F} \times 100 \qquad (13)$$

Where:

OL: mass of obtained lipids (g)

F: mass of feedstock (g)

Lipids extracted were further analyzed by HPLC-SEC to identify the selectivity to mono, di and tri-glycerides (MDTG) and FFA. Tetrahydrofuran was used as an eluent. In a typical measurement, 2-3 droplets of a sample were pipetted into a 12 mL vial and weighed and filled with 10 mL tetrahydrofuran. The sample concentration was in the range of 1.5-3.0 mg/mL. The samples were analyzed and quantified by known concentrations of calibration samples of soybean oil.

The prepared samples were filtered with 0.2 μm syringe filters (containing a PTFE membrane). The samples were then analyzed by HPLC-SEC system composed of a LT-ELS-detector (Low Temperature Evaporative Light-Scattering Detector, Sedex 85, Sedere LT-ELS-detector) with addition components including degasser (DGU-14A), the gradient pump (FCV-10ALVP), the fraction collector (Pharmacia LKB-HeliFrac) and the system controller (SCL-10AVP). HPLC-SEC also equipped three different columns two similar Jordi Gel DVB 500a (300 mm × 7.8 mm) and one Guard column (50 × 7.8 mm). Two similar columns were used to get a better separation. These three columns were used for separation of components and the peaks were measured with an integrator Shimadzu Class- VP 8v.6.12 SP5.

In general, higher molecular components would elute faster than lighter molecular compounds. Typically, the detected components eluted in the following order triglycerides, diglycerides, monoglycerides, FFA and sterols. A typical SEC chromatogram of lipid samples extracted with supercritical hexane at reaction conditions of 2 h and 600 rpm is shown in Figure 9. It is noteworthy that a large number of samples should be analyzed in the same day to achieve representative data.

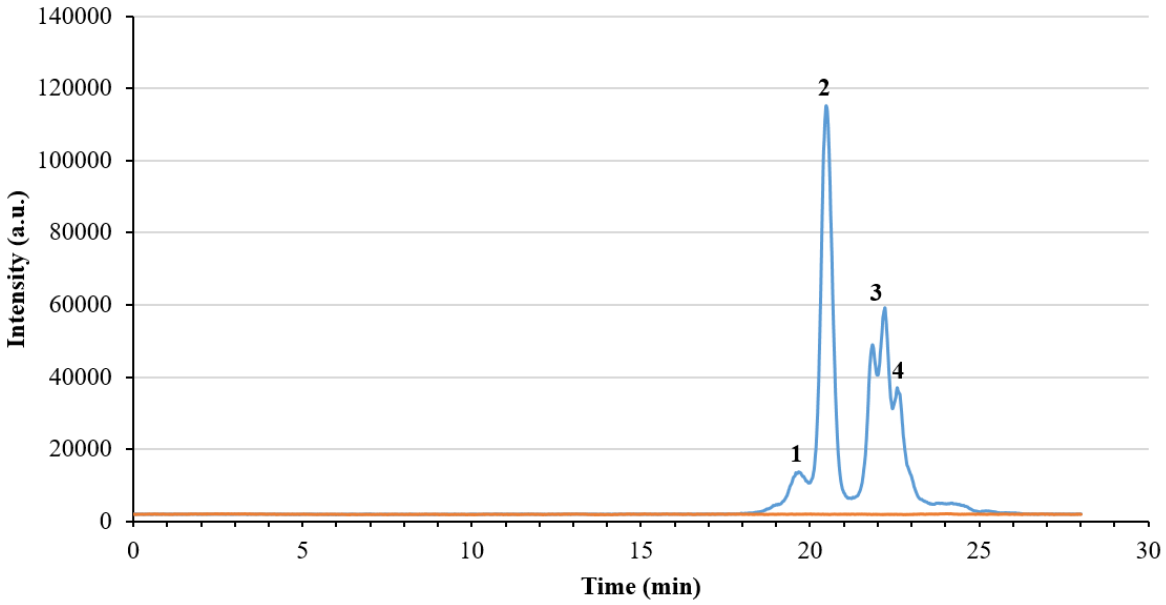

Figure 9. The SEC chromatogram of the lipids extracted from *Chrollela* algae with supercritical hexane after 2 h extraction time with 300 rpm (blue curve). Notation: (1) and (2) triglycerides and diglycerides with the retention time of 19.6 and 20.5 min, respectively, (3) monoglycerides and FFA with the retention time 22-22.5 min, (4) sterols with the retention time > 22.5 min.

The amounts of MDTG and FFA were calculated using a calibration curve of soybean oil. The selectivity to MDTG and FFA was calculated with the following equation

$$S[\%] = \frac{MDTG+FFA}{OL} \times 100 \qquad (14)$$

Where

MDTG: mass of mono, di and tri-glycerides and FFA (g)

OL: mass of obtained lipids (g)

In order to obtain fatty acids profile of the extracted lipids, the lipid sample was hydrolyzed by sulfuric acid as described by Li-Beisson et al. with modification (Li-Beisson et al., 2013, p.33). The transesterified sample was silylated as described in Section 2.8.1 before being analyzed by GC-MS and GC-FID. In a typical measurement, 100 mg extracted lipids were placed in an 8 mL vial and filled by 2 mL of 2.5% H_2SO_4 in methanol (v/v). Thereafter the sample was heated in an oven at 80 °C for 1 h. Afterwards, the sample was naturally cooled to room temperature. 2 mL of pentane was added into the vial followed by 0.9% NaCl (w/v) to extract FAME. The vial should be vigorously shaken and the phases were separated by a centrifuge. The upper layer-FAME fraction in pentane was carefully transferred into another

vial. FAME was concentrated by evaporation of pentane and dissolved by dodecane in a 10 mL volumetric flask prior to the analysis by GC-MS and GC-FID. The preparation procedure for GC-MS and GC-FID analysis was described in Section 2.8.1.

2.7.3 Chlorophylls and carotenoids measurements

As chlorophylls and carotenoids which are non-polar lipids could be extracted together with MDTG and FFA, the measurement of their concentration is essential. Chlorophylls a and b and carotenoids were determined by a method described in by Wellburn (Wellburn, 1994). Two droplets of lipids sample were pipetted into 12 mL vial and weighed and dissolved in 10 mL 80% acetone (80% acetone and 20% deionized water). The sample concentration was in the range of 1-1.7 mg/mL. The diluted samples were scanned from 400 to 800 nm with a sample interval of 0.1 nm using a Shimadzu UV-2550 UV-Vis Spectrophotometer. The determination of Chlorophyll a and b and carotenoids for 80% acetone as a solvent was done as follows

$$\text{Chlorophyll a (Ca)}(\mu g/mL) = 12.25A663.2 - 2.79A646.8 \quad (15)$$

$$\text{Chlorophyll b } (C_b)(\mu g/mL) = 21.5A_{646.8} - 5.1A_{663.2} \quad (16)$$

$$\text{Total carotenoids } (C_{x+c})(\mu g/mL) = (1000A_{471}\text{-}1.82C_a - 85.02C_b)/198 \quad (17)$$

2.7.4 Thermogravimetric analysis

The thermogravimetric analysis (TGA) was performed by a Pyris-TGA, Perkin Elmer instrument under nitrogen flow of 20 mL/min to avoid oxidation of sample. The lipid sample was inserted in a platinum pan and heated from 25-800 °C in synthetic air.

2.7.5 Scanning electron microscopy analysis and EDXA-analysis

The morphology of solid samples was determined by a Zeiss Leo 1530 Gemini scanning electron microscope instrument equipped with a ThermoNORAN vantage X-ray detector. The energy dispersive X-ray analysis was also performed with the same instrument.

2.7.6 Fourier transform infrared spectroscopy (FTIR)

The infrared spectrometry analysis was performed with an ATI Mattson FTIR. A drop of the *Chlorella* sample was placed between two thin KBr disks. The spectrum was recorded in the range 4000-400 cm^{-1} with a resolution of 2 cm^{-1} using 64 scans per second.

2.7.7 Organic elemental analysis

The quantification for organic elements including N, C, H and S was carried out for lipid sample using an Organic elemental analyzer Flash 2000 from Thermo Scientific. The duplicate measurements were performed. In a typical measurement, approximately 2 mg of samples and standards were carefully weight into tin cups. The measurement was carried out under He and O_2. Methionine was used as a calibration standard, while sulfanilamide was used as a check standard. The standards were purchased from Elemental Microanalysis Limited.

3 RESULTS AND DISCUSSIONS

3.1 Validation of the GC method

The results show that a range of concentrations between 1-10 mg/mL injected to chromatograph is within detection limit. It is confirmed by the linearity of mass and area without breakthrough points detected shown in Figure 10. In addition, the deviation of RF of each component is acceptable.

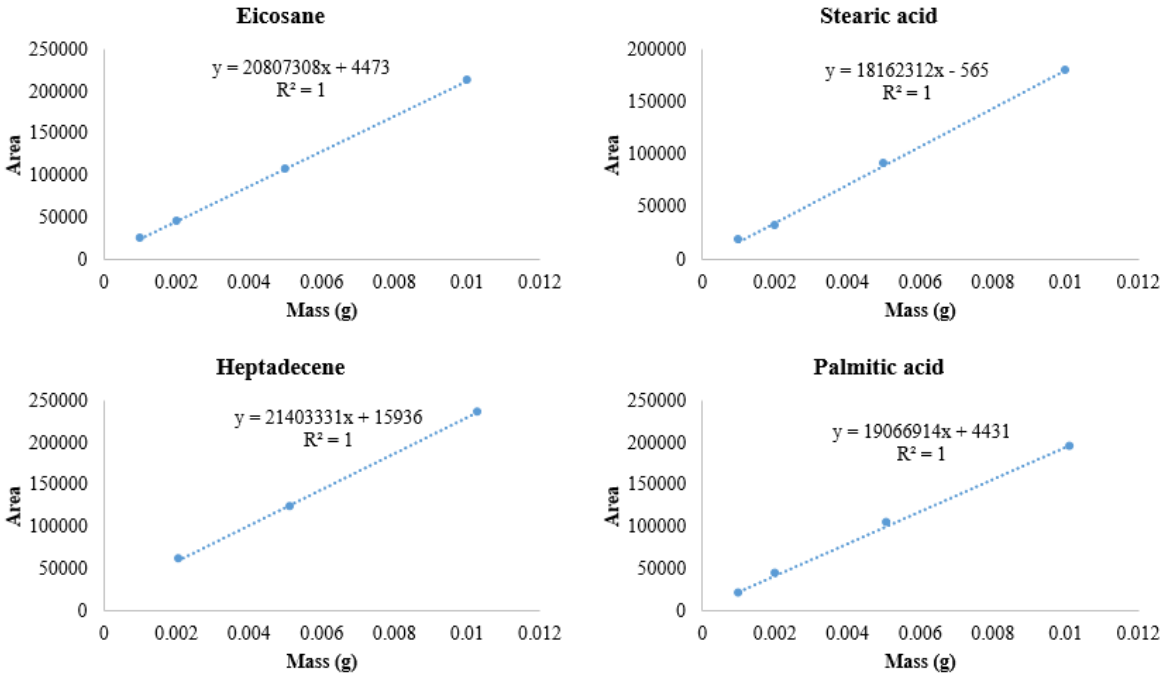

Figure 10. Validation of the internal standard method for various components

3.2 Catalyst characterization

The synthesized Ni catalyst supported on H-Y-80 and SiO_2 were characterized in our laboratory. The characterization techniques for determination of physicochemical properties

of materials used in the current work were inductively coupled plasma-optical emission spectroscopy (ICP-OES), nitrogen physisorption (BET), transmission electron microscopy (TEM), temperature-programmed reduction (TPR), temperature-programmed desorption of ammonia (NH_3-TPD) and carbon dioxide (CO_2-TPD).

Ni content in the fresh catalysts was confirmed by ICP-OES to be 4.9 wt% which is in excellent agreement with the nominal content of 5 wt%. In addition, determination of specific surface area was made as presented in Table 3. 5 wt% Ni/H-Y-80 has the largest specific surface area of 660 m^2 /g, which decreased compared to the neat H-Y zeolite which specific surface area is 995 m^2 /g. The apparent pore diameter increased from 0.97 nm to 1.81 nm after impregnation of nickel which can be explained by blocking of narrow pores with nickel clusters (Hachemi et al., 2016). The specific surface area of 5 wt% Ni/H-Y-80 in the current study is quite similar to the findings of Zuo et al. (Zuo et al., 2012) who used 7 wt% Ni/HY used in HDO of methyl palmitate with the specific surface area of 616.9 m^2 /g. 5 wt% Ni/SiO_2 exhibited a smaller specific surface area of 590 m^2 /g and the pore diameter of 1.44 nm.

Table 3. Physical properties of the fresh catalysts

	Support particle size (μm)	**Specific surface area (m^2 /g)**	**Pore volume (cm^3/g)**	**Average pore diameter (nm)**
H-Y-80	<63	995	0.32	0.97
5 wt% Ni/H-Y-80	<63	660	0.22	1.81
5 wt% Ni/SiO_2	40-63	590	0.12	1.44

The average metal particle size was calculated based on TEM images as shown in Figure 11. The average metal particle size of 5 wt% Ni/H-Y-80 being 4 nm is very similar to the data of Song et al, who studied the importance of Ni particle size and distribution on hydrodeoxygenation of microalgal oil. It has been reported (Song, Zhao and Lercher, 2013) that small and uniform metal particle size resulted in high initial activity and high catalyst stability.

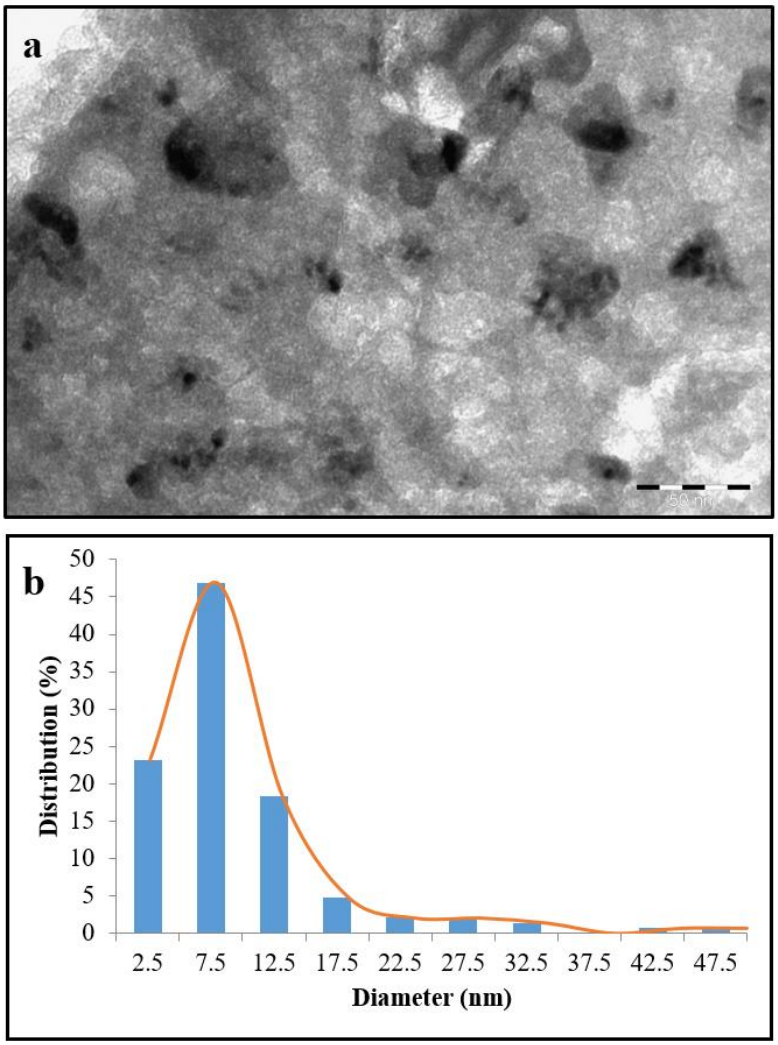

Figure 11. (a) TEM image and (b) metal particle size distribution of the fresh 5 wt% Ni/H-Y-80

Temperature-programmed desorption of NH_3 and CO_2 was performed to determine acidity and basicity, respectively, of the fresh H-Y-80 and 5 wt% Ni/H-Y-80 catalysts. As presented in Table 4, a slight decrease of acidity was observed for 5 wt% Ni/H-Y-80 compared to the fresh zeolite. On the other hand, the parent zeolite exhibited higher basicity than the metal modified catalyst (Hachemi et al., 2016).

Table 4. NH_3 and CO_2 uptakes of the fresh zeolite and the fresh nickel catalyst

	NH_3 uptake (mmol/g)	CO_2 uptake (mmol/g)
	Total acidity	Total basicity
H-Y-80	0.51	38.3
5 wt% Ni/H-Y-80	0.42	33.9

3.3 Lipid extraction

3.3.1 Effect of the extraction time using supercritical hexane as a solvent

In order to study the effect of extraction time, supercritical lipid extraction using hexane as a solvent was performed at different time of 5, 10, 20, 30, 60, 120 and 360 min. The temperature and stirring speed were set to 235 °C and 300-320 rpm, respectively. The result shows that the longer extraction time, the higher is the yield of lipids, increasing 6 times after 2 hours as shown in Figure 12. The yield of approximately 10% remained nearly constant even when the extraction time was prolonged up to 6 hours. This value is close to the theoretical yield of approximately 12% (the lipids content provided by a manufacturer). Figure 12 presents the yield of lipids extracted from *Chlorella* algae at different reaction times. The calculation was made for 2 samples of duplicate supercritical lipid extractions.

The lipids samples obtained at different extraction times were then analyzed by SEC to identify the selectivity to mono, di and tri-glycerides (MDTG) and FFA. The analysis showed that the selectivity to these components decreased when the reaction time increased as presented in Figure 12. The reason is that longer extraction time could efficiently break the cell walls of algae, however, also other non-polar lipids (such as chlorophyll and carotenoids) and non-polar fractions could be extracted together with MDTG and FFA.

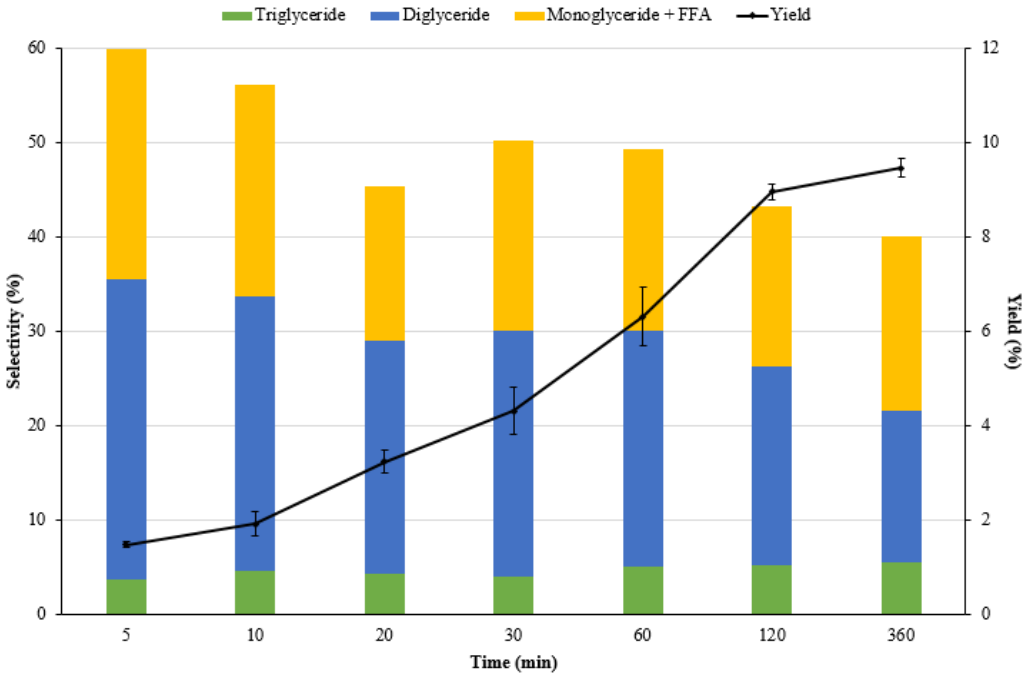

Figure 12. The selectivity to MDTG, FFA and lipids yield at different extraction times in supercritical hexane extraction from *Chlorella* algae. Conditions: 5 g algae, 100 mL hexane, 235 °C, 34 bar and 300 rpm stirring speed

In addition to MDTG and FFA, chlorophyll a and b and total carotenoids were determined by UV-Vis Spectroscopy. As presented in Figure 13, prolonging the duration of extraction could lead to the decrease of chlorophyll a and b. Due to low lipid yields in the range of 0.014-0.02 lipids/g algae extracted at 5 and 10 min, the presence of even small amounts of chlorophyll a and b in the extract could lead to their high concentration. Because of this reason, the standard deviation of chlorophyll a, for example, has a wide fluctuation. Meanwhile, the concentration of total carotenoids seems to be constant. The average concentration of chlorophyll a in the current work is approximately 1000 μg/g, which is probably similar to the one obtained by Iqbal and Theegala who used *Nannochloropsis* sp. (Iqbal and Theegala, 2013).

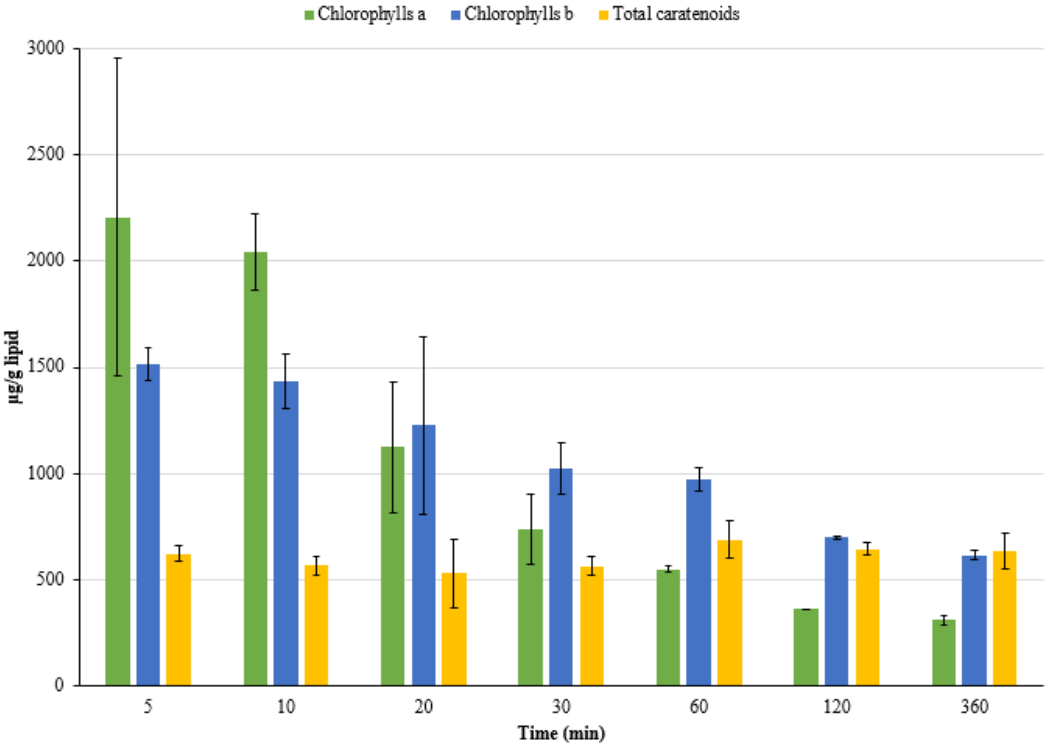

Figure 13. Pigments (chlorophylls and carotenoids) concentration at different extraction times in supercritical hexane extraction from *Chlorella* algae. Conditions: 5 g algae, 100 mL hexane, 235 °C, 34 bar and 300 rpm stirring speed.

3.3.2 Effect of stirring speed

The effect of agitation was investigated at three different speeds of 300, 600 and 1200 rpm. In a previous study, 300 rpm was set as a stirring speed for lipids extraction from *Scenedesmus sp.* with supercritical hexane (Shin et al., 2014). The temperature was still set to 235 °C, while experimental duration was 2 h. Figure 14 shows the yield of lipids at different stirring speed in the current study. Interestingly, the higher was the stirring speed, the lower was the yield of lipids. In fact, the yield of lipids decreased approximately by 30% when stirring speed reached 1200 rpm. The fall in the yield at high stirring speed is attributed to low diffusion of lipids, which happens across the cell wall, since diffusive extraction is an influencing factor for lipid extraction and is dependent on the magnitude or intensity of bulk convection in the media (Ranjan, Patil and Moholkar, 2010). In addition, a gentle stirring speed has been found to accelerate cell lysis and to enhance extraction efficiencies (Yang et al., 2014). The calculation was made on duplicate samples for supercritical lipid extraction.

SEC analysis was conducted to investigate selectivity to MDTG and FFA of lipids samples extracted with supercritical hexane using different stirring speeds. The results show that higher selectivity was observed with higher stirring speeds of 600 and 1200 rpm compared to that at 300 rpm. A higher selectivity was attributed to a lower yield of lipids. At low stirring speed of 300 rpm, non-polar components seem to be extracted efficiently. A higher amount of impurities was obtained as a result. On the other hand, MDTG and FFA were predominantly extracted and the impurities were only extracted to a minor extent not favorable with less interaction between algae and solvent at rapid agitation.

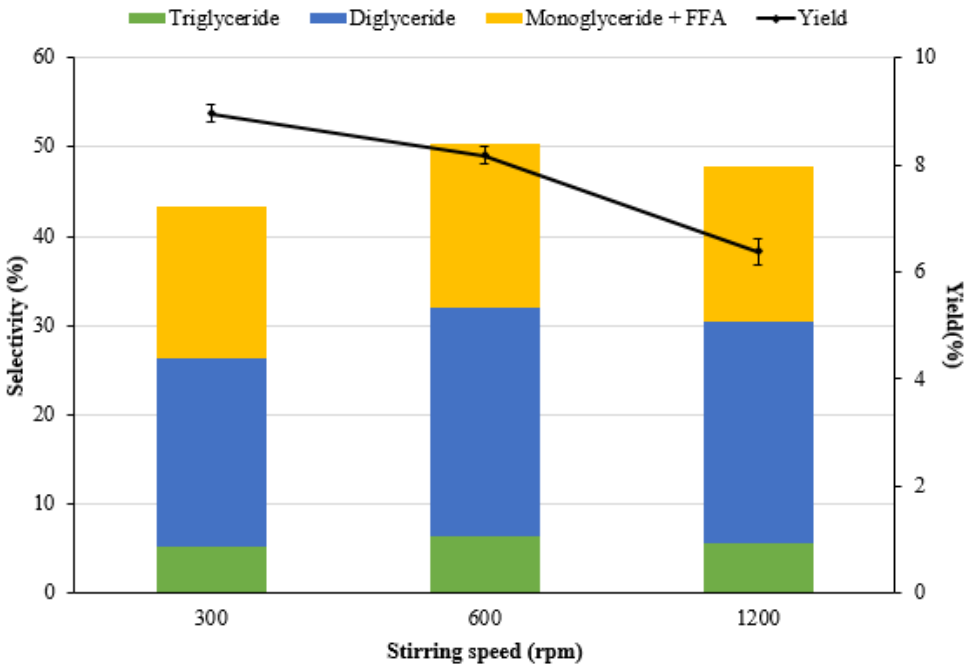

Figure 14. The selectivity to MDTG and FFA and lipids yield at different stirring speeds in supercritical hexane extraction from *Chlorella* algae. Conditions: 5 g algae, 100 mL hexane, 235 °C, 34 bar and 2 h extraction time.

The difference in the concentrations of chlorophyll a and b at different agitation is not significant. Total carotenoids concentration, however, decreases slightly with increasing stirring speed as shown in Figure 15.

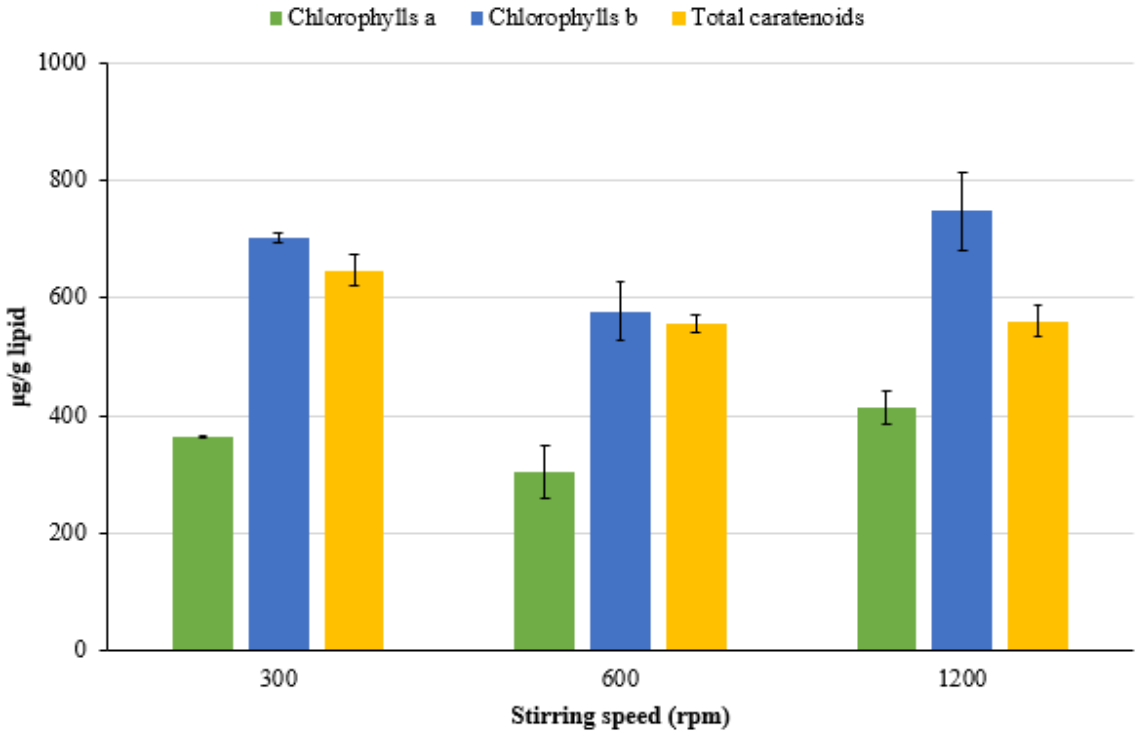

Figure 15. Concentration of pigments (chlorophylls and carotenoids) in the lipid sample at different stirring speeds in supercritical hexane extraction from *Chlorella* algae. Conditions: 5 g algae, 100 mL hexane, 235 °C, 34 bar and 2 h extraction time

The lipids yield of 8.96% obtained at optimum conditions of 300 rpm for 2 h (HCH-2-300) is lower than that in the previous finding in ref (Shin et al., 2014) when *Scenedesmus* sp. was also extracted by supercritical hexane. Higher lipids yield obtain in ref (Shin et al., 2014) can be attributed to a higher lipid content of *Scededesmus* algae species which could be up to 40% (Trivedi et al., 2015).

The *Chlorella* and *Scenedesmus* and *Nannochloropsis* algae species belong to a group of thick-cell wall algae species. This might cause difficulties in their lipid extraction (Borowitzka, 2013, p.80). An efficiency of cell disruption was analyzed by comparison of TEM analyses for raw algae and solid residues after being treated by supercritical hexane at 300 rpm for 2 h. As shown in Figure 16, intact cell walls and intracellular organs could be clearly seen for fresh *Chlorella* (Figure 16a), whereas, only cell walls were observed

confirming the diffusive extraction (Figure 16b). For the same sample of the treated algae, an interesting finding was witnessed namely that the cell walls seemed to collapse together forming coke which mainly remained after extraction (Figure 16c). This is understandable as algae was treated at high temperature and pressure of 235 °C and 34 bar, respectively. The results in the current work is similar to the one obtained in ref. (Chen et al., 2012), in which subcritical co-solvents (hexane and ethanol) was used to extract lipids from microalgae pastes of *Nannochloropsis* sp; after extraction, the algal cell shrunken, collapsed and some microholes were formed. The image of extracted algae residue in Figure 16b might be considered as treated algae at an intermediate extraction stage and the coke was formed as a final treatment when the holes were nearly destructed as seen in Figure 16c.

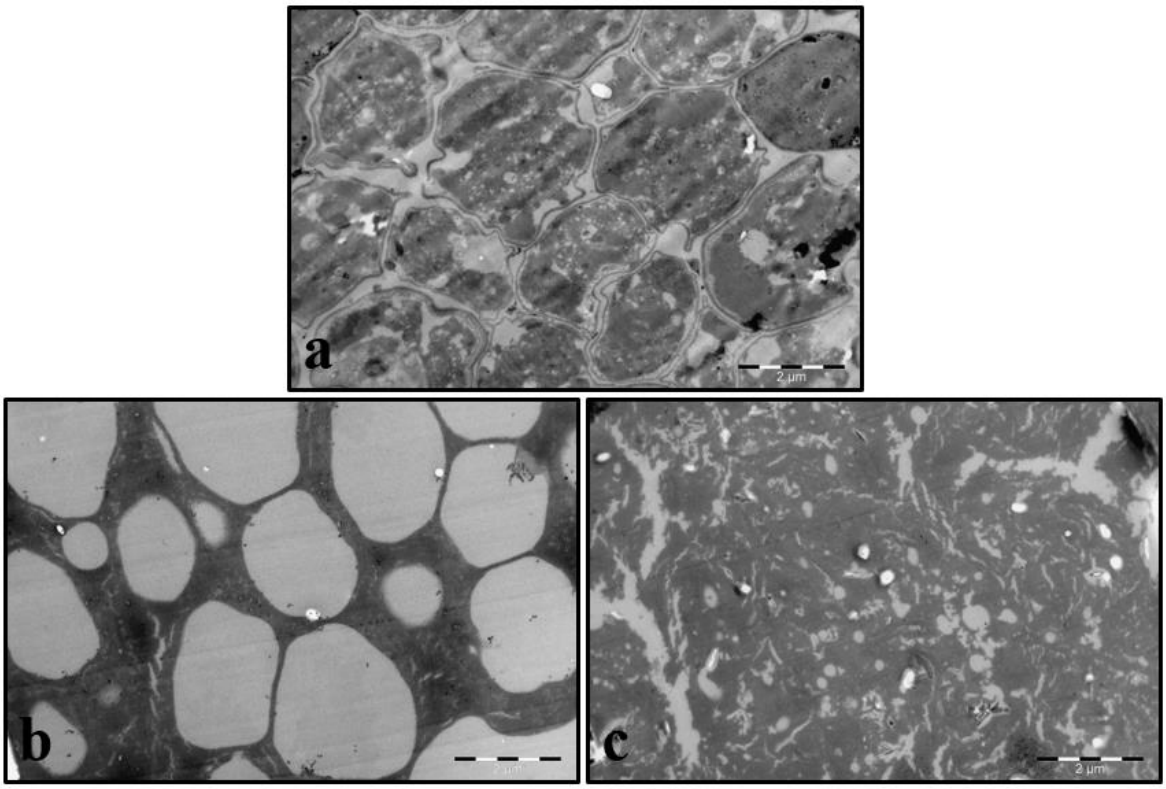

Figure 16. Transmission electron microscopy images of *Chlorella* samples (a) Fresh *Chlorella*, (b) and (c) Treated *Chlorella* by supercritical hexane at 300 rpm for 2 h.

3.3.3 Characterization of lipid sample produced via supercritical hexane extraction

The lipid sample produced via supercritical hexane extraction at optimum conditions of 2 h and 300 rpm (HCH-2-300) was transesterified according to the procedure described in Section 2.8.2 and analyzed by GC-MS and GC-FID for identification and quantification of

fatty acid profile, respectively. Figure 17 presents the chromatograms of HCH-2-300 analyzed by GC-MS. Additionally, Table 5 shows the percentage of fatty acid components in HCH-2-300 which have been derived from the corresponding FAME shown in Figure 17. As presented in Table 5, the unsaturated fatty acids are the main components being approximately 68%. The high content of unsaturated fatty acids is quite similar to the one obtained in ref. (Viêgas et al., 2015) where nearly 65% unsaturated fatty acids were obtained from another *Chlorella* alga from China.

The fatty acid yield in the current work of 4.8% is nearly twofold lower than that obtained in the finding of Shin et al. who used supercritical hexane to extract lipids from *Scenedesmus* sp. algae (Shin et al., 2014). It is understandable since the lipid content in *Scenedesmus* species could reach up to 40% (Trivedi et al., 2015). However, the fatty acid yield is quite similar to the one obtained by Olkiewicz et al. (Olkiewicz et al., 2015) who used hydrated phosphonium ionic liquid for lipid extraction from *Chlorella vulgaris.*

Table 5. Fatty acid profile of the extracted lipid sample HCH-2-300

Crude lipids yield (% algae)	8.96 ± 0.17
Fatty acids composition (% FAME)	
Myristic acid (C14:0)	1.03
7,10-hexadecadienoic acid (C16:2)	0.38
7,10,13-hexadecatrienoic acid (C16:3)	9.37
9-hexadecenoic acid (C16:1)	11.69
Hexadecanoic acid (C16:0)	22.35
15-methyl hexadecanoic acid methyl ester (C17:0)	0.66
Cis-10-heptadecenoic acid (C17:1)	0.58
Heptadecanoic acid (C17:0)	3.88
Linoleic acid (C18:2)	42.81
Oleic acid (C18:1)	3.06
Stearic acid (C18:0)	4.19
Fatty acids content (%)	53.59 ± 0.17
Fatty acid yield[a] (wt.%)	4.8

[a] fatty acid yield (wt.%) = yield of crude lipids (wt.%) × fatty acid content (%)/100

All measurements were made in duplicate and the standard deviation was calculated.

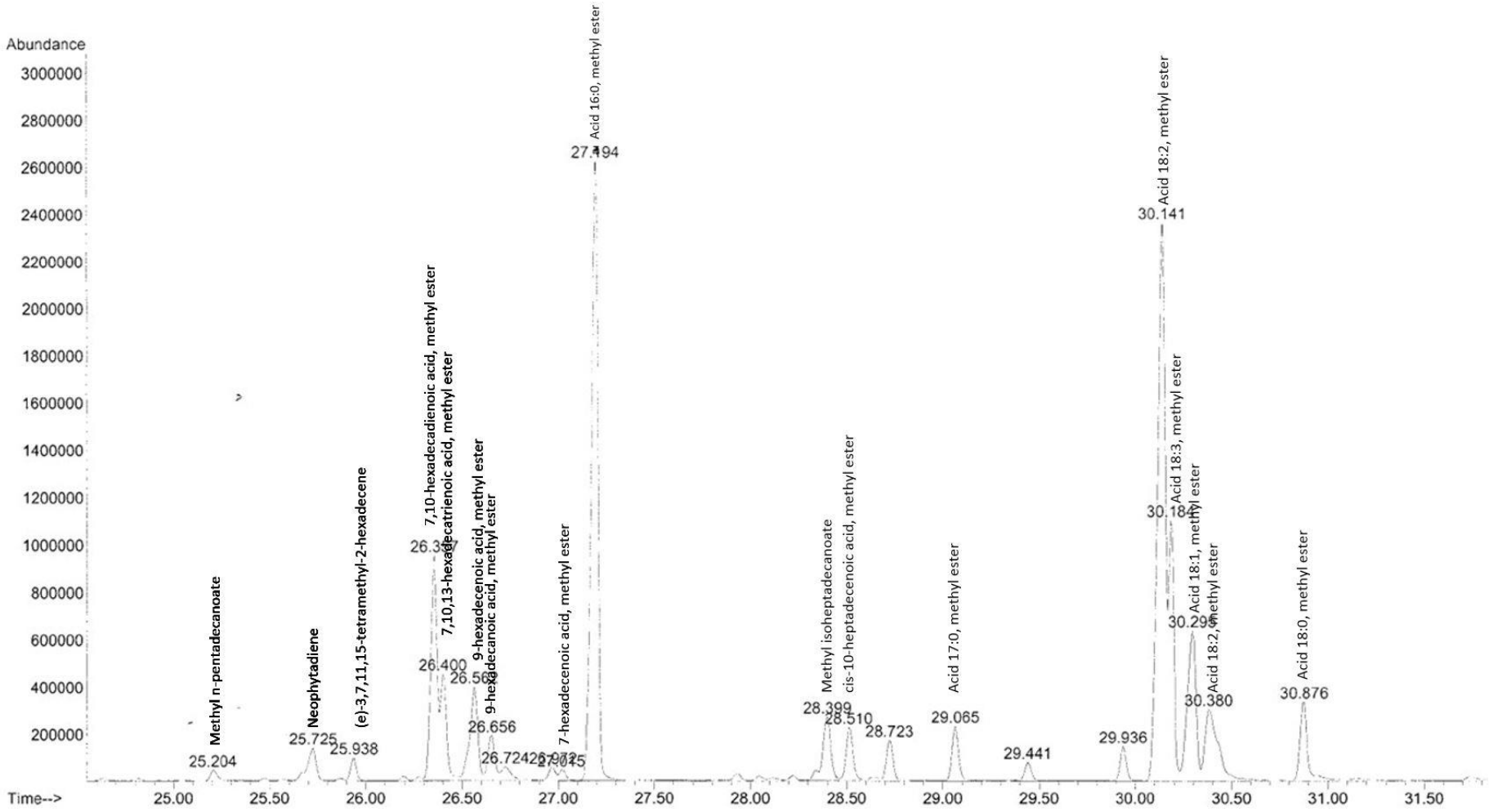

Figure 17. A chromatogram of the extracted lipid sample HCH-2-300 analyzed by GC-MS

In addition to GC and SEC analyses, the HCH-2-300 lipid sample was also analyzed by FTIR. As shown in Figure 18, FTIR displays peaks corresponding to various bond vibrations in lipids at wavenumber of 3008, 2954, 2925, 2854 and 1739 cm^{-1}. The obtained result is quite similar to other studied as presented in Table 6. More importantly, it is consistent with SEC and GC analysis results, in which most of the components observed were MDTG and FFA, respectively, corresponding to the total yield of fatty acids of 5 wt%. Other components such as polysaccharides, carbohydrates and amides were also identified in HCH-2-300 sample.

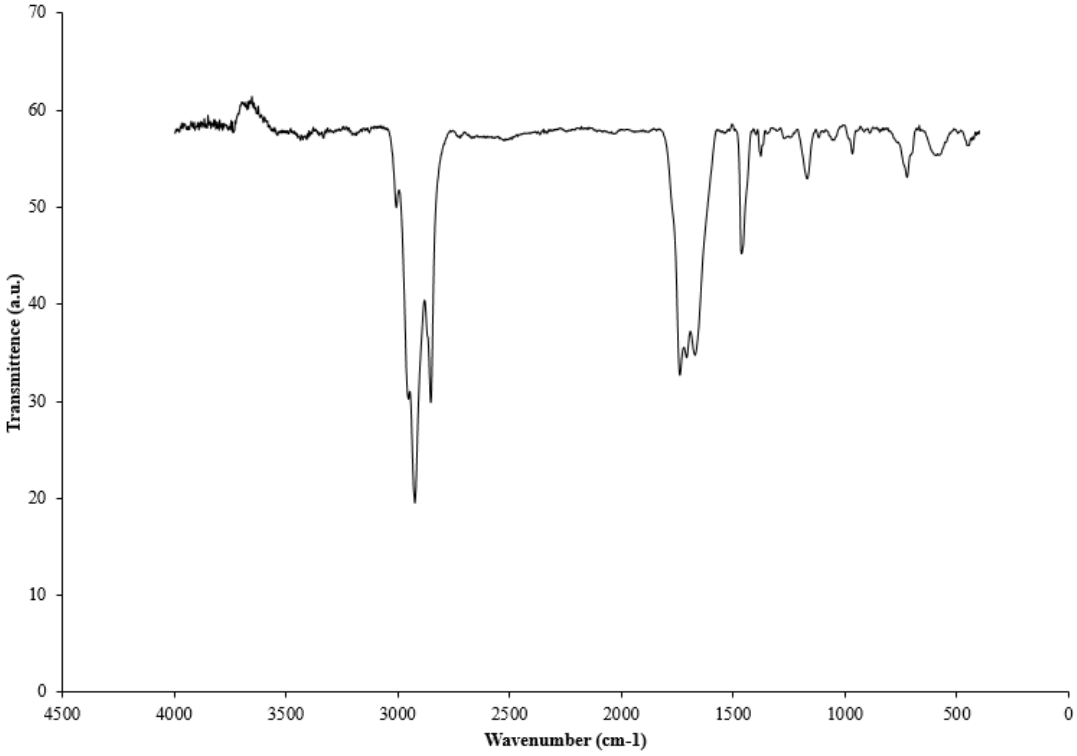

Figure 18. FTIR from the extracted lipid sample HCH-2-300

Table 6. Frequencies and band assignments for FTIR obtained from the extracted lipid sample HCH-2-300

Main peak (cm^{-1})	**Assignment**	**Component**	**Wavenumber range (cm^{-1})**	**Reference**
3008	$\nu_{as}CH_2$	Lipids	2809-3012	(Liu, Mukherjee, Hawkes and Wilkinson, 2013)
2954	$\nu_{as}CH_2/\nu_{as}CH_3$	Lipids	2809-3012	(Benning, Phoenix, Yee and Tobin, 2004; Dean, Martin and Sigee, 2007)
2925	$\nu_{as}CH_2$	Lipids	2809-3012	(Benning et al., 2004; Liu et al., 2013; Ponnuswamy, Madhavan and Shabudeen, 2013)
2854	$\nu_{as}CH_2$	Lipids	2809-3012	(Liu et al., 2013)
1739	ν(C=O)	Lipids	1745-1734	(Dean, Martin and Sigee, 2007; Liu et al., 2013)
1708	ν(C=O)	Esters		(Benning et al., 2004)
1671	ν(C=O)	Protein (Amide I)	1538-1709	(Ponnuswamy, Madhavan and Shabudeen, 2013)
1461	$\nu_{as}CH_2$	Protein (Amide III)		(Dean, Martin and Sigee, 2007; Benning et al., 2004)
1378	ν_s(C-O)	Carboxylic acids		(Benning et al., 2004; Dean, Martin and Sigee, 2007)
1273	ν_{as}(P=O)	Nucleic acids, Phosphoryl groups	1191-1356	(Liu et al., 2013; Ponnuswamy, Madhavan and Shabudeen, 2013)
1173	ν(C-O-C)/ν_{as}(P=O)	Polysaccharides	1200-900	(Liu et al., 2013; Benning et al., 2004)
968	ν(C-O-C)/ν_{as}(P=O)	Polysaccharides	1200-900	(Liu et al., 2013; Benning et al., 2004)

The organic elemental analysis (OEA) showed that carbon and hydrogen are the main components in the lipid sample HCH-2-300 as shown in Table 7, which displays 2 measurements along with the average. The high content of carbon could result in a high heating value. On the other hand, the sulfur content higher than a maximum limit of 50 ppm (0.005%) for sulfur in diesel in EU might be unfavorable for biofuel production used in diesel engine without hydrodesulfurization. Small amounts of nitrogen represent proteins which were also observed by FTIR.

Table 7. The elemental composition of lipid sample (HCH-2-300)

Element	**Experiment 1 (%)**	**Experiment 2 (%)**	**Amount (% ± SD)**
C	71.95	72.50	72.22 ± 0.387
H	10.92	10.97	10.94 ± 0.040
N	3.96	4.07	4.01 ± 0.076
S	0.26	0.24	0.25 ± 0.014

Thermogravimetric analysis was performed for the lipid sample (HCH-2-300) as shown in Figure 19. HCH-2-300 lipid sample exhibited three decomposition stages. The first stage released 15-20% of total volatiles components ranging from 170-250 °C which may represent aldehydes and ketones (Kebelmann, Hornung, Karsten and Griffiths, 2013), potentially formed during extraction via autoxidation. The second stage within 250-500 °C released over 60% of the volatiles which may represent fatty acids components. Two main peaks were detected at 350 °C and 400 °C in HCH-2-300 lipid sample. It is consistent with the results measured by SEC and UV-Vis for MDTG, FFA, chlorophylls and total carotenoids, where 60% of these component were detected. The final stage ranging 500-800 °C released 5% of volatiles and only 0.45% of the char residue was formed. The obtained result was slightly different from the one obtained by Kebelmann et al. (Kebelmann et al., 2013) when the two main peaks were observed at 300 °C and 400 °C and 78% of the volatiles represented fatty acids components.

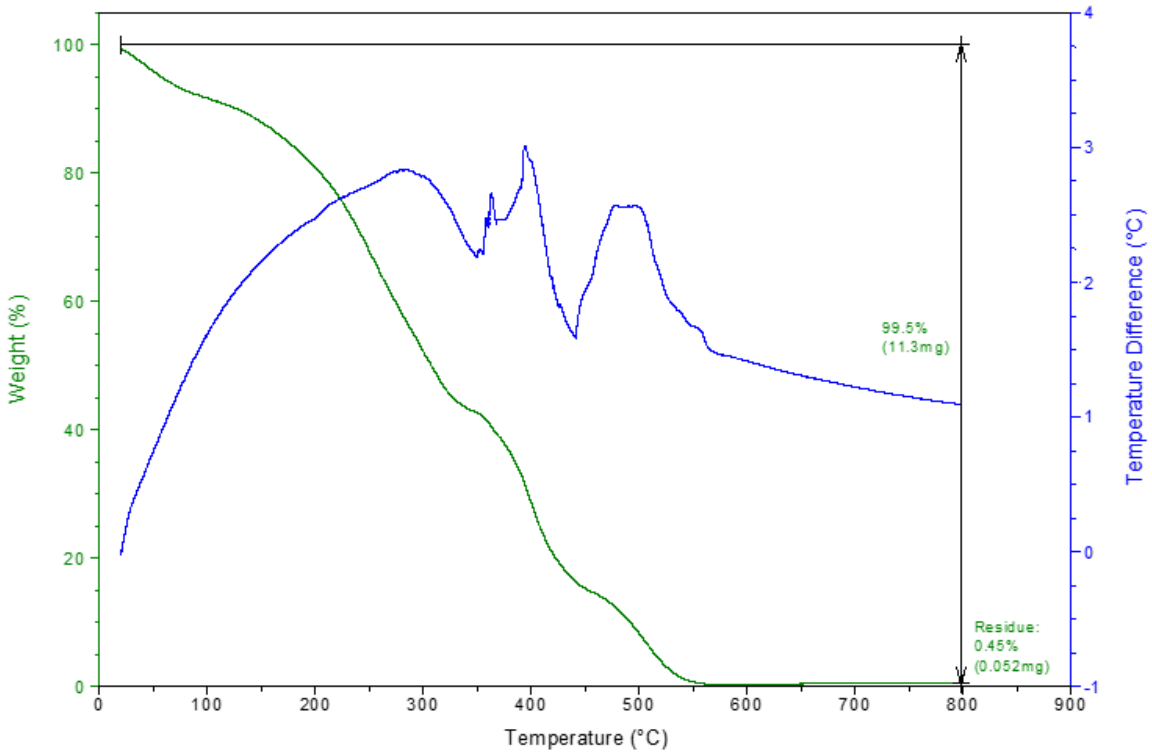

Figure 19. TGA and temperature difference for the lipid sample produced via supercritical hexane extraction at reaction conditions of 2 h and 300 rpm. Notation: weight loss (red) and temperature different (blue)

The char residue formed in TGA analysis was further characterized by EDXA. Four spots on the char residue were randomly chosen for the analysis shown in Figure 20. The results revealed that the background of the char is mainly made from Al_2O_3, since Al and O are the main elements in the char as presented in Table 8. The presence of Mg in the char is understandable since chlorophylls present in lipids contain Mg. In addition, a lower content of Ca is advantageous as this element is a poison for catalytic hydrodeoxygenation.

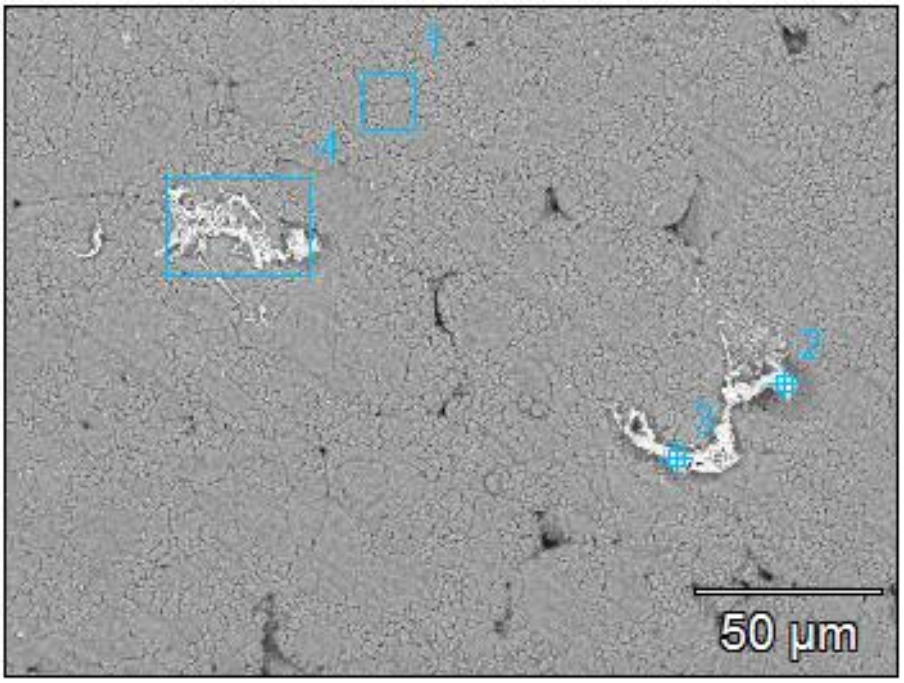

Figure 20. SEM image of the char residue from TGA of the lipid sample HCH-2-300 shown in Figure 19

Table 8. Weight percentage of elements in the char residue of the lipid sample HCH-2-300

Element	O	N	Mg	Al	Si	S	K	Ca	Fe	Zn
Spot 1	47.17 ± 0.47			52.83 ± 0.26						
Spot 2	47.96 ± 0.46	1.34 ± 0.07	0.22 ± 0.06	33.32 ± 0.21	2.38 ± 0.13	2.29 ± 0.06	5.65 ± 0.18	2.69 ± 0.18	4.15 ± 0.35	
Spot 3	48.21 ± 0.46	1.54 ± 0.13	0.33 ± 0.05	28.73 ± 0.19	3.39 ± 0.12	1.65 ± 0.05	6.04 ± 0.16	2.74 ± 0.17	6.06 ± 0.35	1.31 ± 0.37
Spot 4	44.51 ± 0.46	0.74 ± 0.07		44.15 ± 0.23	1.24 ± 0.13	1.76 ± 0.07	3.99 ± 0.19	1.27 ± 0.18	2.35 ± 0.22	

3.4 Hydrodeoxygenation of lipids

Lipids extracted under supercritical hexane at 300 rpm for 2 h were studied in hydrodeoxygenation. Catalysts used in the current work were 5 wt% Ni/H-Y-80 and 5 wt% Ni/SiO_2. A higher conversion of lipids over 5 wt% Ni/H-Y-80 compared to that of 5 wt% Ni/SiO_2 is in accordance with the previous findings in ref (Hachemi et al., 2016). Figure 21a and b show the kinetics of lipids transformation. The concentration of MDTG decreased with time since they were hydrogenated and hydrolyzed to FFA. Meanwhile, the concentration of FFA decreased from 0 to 60 minutes as it was hydrodeoxygenated to hydrocarbons (C15-C18 alkanes). However, it starts raising after 6 h for 5 wt% Ni/H-Y-80, whereas, it decreased slightly for 5 wt% Ni/SiO_2. Simultaneously, the selectivity to C15-C18 is 6.04% and 5.9% for 5 wt% Ni/H-Y-80 and 5 wt% Ni/SiO_2, respectively as presented in Table 9. Compared to a previous study in which microalgae oil extracted from *Nannochloropsis* salina strain was continuously hydrodeoxygenated over 1 wt% Pt/Al_2O_3, 0.5 wt% Rh/Al_2O_3 and presulfided $NiMo/Al_2O_3$ (Zhou and Lawal, 2016), the conversion of this work is low. The lower level of hydrodeoxygenation might be attributed to catalyst deactivation caused by chlorophylls and carotenoids. The transformation of lipids occurs mainly by hydrogenation and hydrolysis with the formation of FFA.

For the comparison of conversion and selectivity hydrodeoxygenation of stearic acid was also performed. Figure 21c reveals that the mass fraction of stearic acid with 5 wt% Ni/H-Y-80 is decreased much faster than those of lipids in case of 5 wt% Ni/H-Y-80 and 5 wt% Ni/SiO_2. It is understandable since the amount of impurities is higher in extracted lipids compared to stearic acid. Transformations of stearic acid were relatively rapid in the first 3 h. As a result, the selectivity to hydrocarbons (C17-C18) is nearly 100%.

Table 9. Conversion and selectivity in hydrodeoxygenation of lipids on 5 wt% Ni/H-Y-80 and 5 wt% Ni/SiO_2 (ID 1 and 2) and stearic acid on 5 wt% Ni/H-Y-80 (ID 3)

		Selectivity after 6h					
ID	**Conversion after 6 h (%)**	**Hydrocarbon (C15-C18) (%)**	**FFA**	**MG**	**DG**	**TG**	**Sterols + Steryl esters**
1	34.96	6.04	56.86	8.69	22.94	2.36	3.11
2	15.25	5.90	41.65	13.49	33.38	2.17	3.42
3	100	99.9	-	-	-	-	-

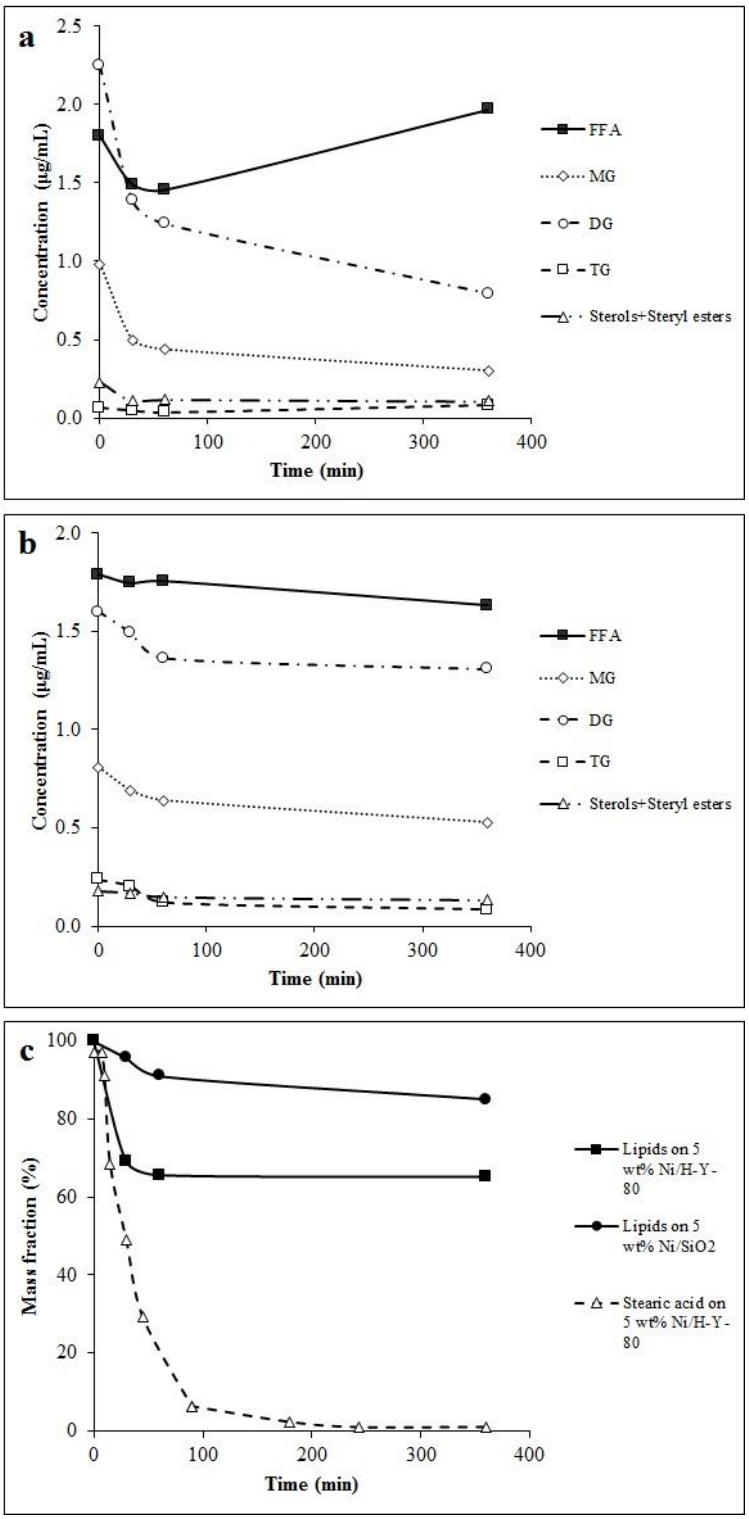

Figure 21. (a), (b) Kinetics of lipid transformations on 5 wt% Ni/H-Y-80 and 5 wt% Ni/SiO_2 and (c) comparative mass fraction of lipids on 5 wt% Ni/H-Y-80 and 5 wt% Ni/SiO_2 and stearic acid on 5 wt% Ni/H-Y-80. Conditions: 1 g reactant and 0.25 g catalyst in 100 mL dodecane, 300 °C, 30 bar total pressure in H_2 and 1200 rpm stirring speed.

4 CONCLUSIONS

Lipids extraction from *Chlorella* algae in supercritical hexane was conducted in the current work varying the extraction time and stirring speed. Such extraction was revealed to be feasible since a lipids yield of 10% was obtained under the optimum conditions of 300 rpm and 2 h duration compared to the total nominal lipid contents of 12%. Furthermore, an environmentally friendly extraction with supercritical hexane is attractive due to easy solvent recovery.

For the first time, hydrodeoxygenation of raw *Chlorella* algal lipid was studied over 5 wt% Ni/H-Y-80 and 5 wt% Ni/SiO_2 at 300 °C and under 30 bar total pressure in H_2. A comparative HDO of stearic acid was carried out under similar conditions. The conversion of lipids was about 35% over 5 wt% Ni/H-Y-80 after 6h, whereas, 5 wt% Ni/SiO_2 was totally deactivated after 60 min giving the conversion level of 15%. As a comparison, complete conversion of stearic acid over 5 wt% Ni/H-Y-80 was achieved in 6 h.

Selectivity of 5 wt% Ni/H-Y-80 and 5 wt% Ni/SiO_2 towards hydrocarbons (C15-C18) in HDO of the algal lipid fraction is low, approximately 6%. The lower activity might be attributed to deactivation of catalysts caused by chlorophylls and carotenoids. Additionally, the transformation of lipids proceeded mostly via hydrogenation and hydrolysis with formation of free fatty acids.

Even though the lipid conversion is rather low, future studies in hydrodeoxygenation of lipids extracted from other algae species having higher lipid content could be proposed. Coke resistant catalyst is more preferable than purification of lipids since MDTG and FFA could be lost during the purification process.

REFERENCES

Barrett, E.P.,, Joyner, L.G., and Halenda, P.P., 1951. The Determination of Pore Volume and Area Distributions in Porous Substances. I. Computations from Nitrogen Isotherms. *Journal of the American Chemical Society*, 73(1), pp.373–380.

Benning, L.G.,, Phoenix, V..,, Yee, N., and Tobin, M.., 2004. Molecular characterization of cyanobacterial silicification using synchrotron infrared micro-spectroscopy. *Geochimica et Cosmochimica Acta*, 68(4), pp.729–741.

Bligh, E.G., and Dyer, W.J., 1959. A rapid method for total lipid extraction and purification. *Can J Biochem Physiol*, 37, pp.911–917.

Borowitzka, M.A., 2013. Algae for Biofuels and Energy. In: A.M. Borowitzka and R.N. Moheimani, eds. Dordrecht: Springer Netherlands, pp.77–89.

Brown, S.H., 2010. Zeolites in Catalysis. In: *Handbook of Green Chemistry*. Wiley-VCH Verlag GmbH & Co. KGaA.

Chen, M.,, Liu, T.,, Chen, X.,, Chen, L.,, Zhang, W.,, Wang, J.,, Gao, L.,, Chen, Y., and Peng, X., 2012. Subcritical co-solvents extraction of lipid from wet microalgae pastes of Nannochloropsis sp. *European Journal of Lipid Science and Technology*, 114(2), pp.205–212.

Cowley, J.M., 2005. Handbook of Microscopy for Nanotechnology. In: N. Yao and Z.L. Wang, eds. Boston, MA: Springer US, pp.455–491.

Dean, A.P.,, Martin, M.C., and Sigee, D.C., 2007. Resolution of codominant phytoplankton species in a eutrophic lake using synchrotron-based Fourier transform infrared spectroscopy. *Phycologia*, 46(2), pp.151–159.

Duan, J.,, Han, J.,, Sun, H.,, Chen, P.,, Lou, H., and Zheng, X., 2012. Diesel-like hydrocarbons obtained by direct hydrodeoxygenation of sunflower oil over Pd/Al-SBA-15 catalysts. *Catalysis Communications*, 17, pp.76–80.

Enweremadu, C.C., and Mbarawa, M.M., 2009. Technical aspects of production and analysis of biodiesel from used cooking oil—A review. *Renewable and Sustainable Energy Reviews*, 13(9), pp.2205–2224.

Goldstein, J.I.,, Newbury, D.E.,, Echlin, P.,, Joy, D.C.,, Lyman, C.E.,, Lifshin, E.,, Sawyer, L., and Michael, J.R., 2003. Introduction. In: *Scanning Electron Microscopy and X-ray*

Microanalysis: Third Edition. Boston, MA: Springer US, pp.1–20.

Hachemi, I.,, Jenistova, K.,, Maki-Arvela, P.,, Kumar, N.,, Eranen, K.,, Hemming, J., and Murzin, D.Y., 2016. Comparative study of sulfur-free nickel and palladium catalysts in hydrodeoxygenation of different fatty acid feedstocks for production of biofuels. *Catalysis Science & Technology*, 6(5), pp.1476–1487.

Iqbal, J., and Theegala, C., 2013. Microwave assisted lipid extraction from microalgae using biodiesel as co-solvent. *Algal Research*, 2(1), pp.34–42.

Kebelmann, K.,, Hornung, A.,, Karsten, U., and Griffiths, G., 2013. Intermediate pyrolysis and product identification by TGA and Py-GC/MS of green microalgae and their extracted protein and lipid components. *Biomass and Bioenergy*, 49, pp.38–48.

Kitson, F.G.,, Larsen, B.S., and McEwen, C.N., 1996. Chapter 1 - What Is GC/MS? BT - Gas Chromatography and Mass Spectrometry. San Diego: Academic Press, pp.3–23.

Kubičková, I.,, Snåre, M.,, Eränen, K.,, Mäki-Arvela, P., and Murzin, D.Y., 2005. Hydrocarbons for diesel fuel via decarboxylation of vegetable oils. *Catalysis Today*, 106(1-4), pp.197–200.

Kumar, P.,, Yenumala, S.R.,, Maity, S.K., and Shee, D., 2014. Kinetics of hydrodeoxygenation of stearic acid using supported nickel catalysts: Effects of supports. *Applied Catalysis A: General*, 471, pp.28–38.

Lee, S.J.,, Yoon, B.-D., and Oh, H.-M., 1998. Rapid method for the determination of lipid from the green alga Botryococcus braunii. *Biotechnology Techniques*, 12(7), pp.553–556.

Leofanti, G.,, Padovan, M.,, Tozzola, G., and Venturelli, B., 1998. Surface area and pore texture of catalysts. *Catalysis Today*, 41(1-3), pp.207–219.

Li, Y.,, Ghasemi Naghdi, F.,, Garg, S.,, Adarme-Vega, T.C.,, Thurecht, K.J.,, Ghafor, W.A.,, Tannock, S., and Schenk, P.M., 2014. A comparative study: the impact of different lipid extraction methods on current microalgal lipid research. *Microbial Cell Factories*, 13(1), pp.1–9.

Li-Beisson, Y.,, Shorrosh, B.,, Beisson, F.,, Andersson, M.X.,, Arondel, V.,, Bates, P.D.,, Baud, S.,, Bird, D.,, DeBono, A.,, Durrett, T.P.,, Franke, R.B.,, Graham, I.A.,, Katayama, K.,, Kelly, A.A.,, Larson, T.,, Markham, J.E.,, Miquel, M.,, Molina, I.,, Nishida, I.,, Rowland, O.,, Samuels, L.,, Schmid, K.M.,, Wada, H.,, Welti, R.,, Xu, C.,, Zallot, R., and Ohlrogge, J., 2013. Acyl-Lipid Metabolism. In: *The Arabidopsis Book*. The American

Society of Plant Biologists, p.e0161.

Liu, J.,, Mukherjee, J.,, Hawkes, J.J., and Wilkinson, S.J., 2013. Optimization of lipid production for algal biodiesel in nitrogen stressed cells of Dunaliella salina using FTIR analysis. *Journal of Chemical Technology & Biotechnology*, 88(10), pp.1807–1814.

Llewellyn, P.L.,, Bloch, E., and Bourrelly, S., 2012. Surface Area/Porosity, Adsorption, Diffusion. In: *Characterization of Solid Materials and Heterogeneous Catalysts*. Wiley-VCH Verlag GmbH & Co. KGaA, pp.853–879.

Mäki-Arvela, P.,, Rozmysłowicz, B.,, Lestari, S.,, Simakova, O.,, Eränen, K.,, Salmi, T., and Murzin, D.Y., 2011. Catalytic Deoxygenation of Tall Oil Fatty Acid over Palladium Supported on Mesoporous Carbon. *Energy & Fuels*, 25(7), pp.2815–2825.

Mariod, A.A.,, Matthäus, B., and Ismail, M., 2011. Comparison of Supercritical Fluid and Hexane Extraction Methods in Extracting Kenaf (Hibiscus cannabinus) Seed Oil Lipids. *Journal of the American Oil Chemists' Society*, 88(7), pp.931–935.

Mouahid, A.,, Crampon, C.,, Toudji, S.-A.A., and Badens, E., 2013. Supercritical CO2 extraction of neutral lipids from microalgae: Experiments and modelling. *The Journal of Supercritical Fluids*, 77, pp.7–16.

Niemantsverdriet, J.W., 2007a. Microscopy and Imaging. In: *Spectroscopy in Catalysis*. Wiley-VCH Verlag GmbH & Co. KGaA, pp.179–216.

Niemantsverdriet, J.W., 2007b. Temperature-Programmed Techniques. In: *Spectroscopy in Catalysis*. Wiley-VCH Verlag GmbH & Co. KGaA, pp.11–38.

Olkiewicz, M.,, Caporgno, M.P.,, Font, J.,, Legrand, J.,, Lepine, O.,, Plechkova, N. V,, Pruvost, J.,, Seddon, K.R., and Bengoa, C., 2015. A novel recovery process for lipids from microalgae for biodiesel production using a hydrated phosphonium ionic liquid. *Green Chem.*, 17(5), pp.2813–2824.

Ponnuswamy, I.,, Madhavan, S., and Shabudeen, S., 2013. Isolation and characterization of green microalgae for carbon sequestration, waste water treatment and bio-fuel production. *Int. J. Bio-Sci. Bio-Technol*, 5, pp.17–26.

Rakić, V., and Damjanović, L., 2013. Temperature-Programmed Desorption (TPD) Methods. In: A. Auroux, ed., *Calorimetry and Thermal Methods in Catalysis*. Berlin, Heidelberg: Springer Berlin Heidelberg, pp.131–174.

Ranjan, A.,, Patil, C., and Moholkar, V.S., 2010. Mechanistic Assessment of Microalgal Lipid Extraction. *Industrial & Engineering Chemistry Research*, 49(6), pp.2979–2985.

Rao, L., 2007. Solid acid catalysts in Green Chemistry. *Resonance*, 12(10), pp.30–36.

Rochow, T.G., and Tucker, P.A., 1994. Transmission Electron Microscopy and Electron Diffraction. In: *Introduction to Microscopy by Means of Light, Electrons, X Rays, or Acoustics*. Boston, MA: Springer US, pp.265–296.

Santillan-Jimenez, E., and Crocker, M., 2012. Catalytic deoxygenation of fatty acids and their derivatives to hydrocarbon fuels via decarboxylation/decarbonylation. *Journal of Chemical Technology & Biotechnology*, 87(8), pp.1041–1050.

Searchinger, T.D.,, Hamburg, S.P.,, Melillo, J.,, Chameides, W.,, Havlik, P.,, Kammen, D.M.,, Likens, G.E.,, Lubowski, R.N.,, Obersteiner, M.,, Oppenheimer, M.,, Philip Robertson, G.,, Schlesinger, W.H., and David Tilman, G., 2009. Fixing a Critical Climate Accounting Error. *Science*, 326(5952), pp.527–528.

Sheldon, R.A.,, Arends, I.W.C.E., and Hanefeld, U., 2007. Solid Acids and Bases as Catalysts. In: *Green Chemistry and Catalysis*. Wiley-VCH Verlag GmbH & Co. KGaA, pp.49–90.

Shin, H.-Y.,, Ryu, J.-H.,, Bae, S.-Y.,, Crofcheck, C., and Crocker, M., 2014. Lipid extraction from Scenedesmus sp. microalgae for biodiesel production using hot compressed hexane. *Fuel*, 130, pp.66–69.

Simon-Masseron, A.,, Marques, J.P.,, Lopes, J.M.,, Ribeiro, F.R.,, Gener, I., and Guisnet, M., 2007. Influence of the Si/Al ratio and crystal size on the acidity and activity of HBEA zeolites. *Applied Catalysis A: General*, 316(1), pp.75–82.

Sing, K., 2001. The use of nitrogen adsorption for the characterisation of porous materials. *Colloids and Surfaces A: Physicochemical and Engineering Aspects*, 187-188, pp.3–9.

Snåre, M.,, Kubičková, I.,, Mäki-Arvela, P.,, Eränen, K., and Murzin, D.Y., 2006. Heterogeneous Catalytic Deoxygenation of Stearic Acid for Production of Biodiesel. *Industrial & Engineering Chemistry Research*, 45(16), pp.5708–5715.

Song, W.,, Zhao, C., and Lercher, J.A., 2013. Importance of size and distribution of Ni nanoparticles for the hydrodeoxygenation of microalgae oil. *Chemistry (Weinheim an der Bergstrasse, Germany)*, 19(30), pp.9833–42.

Taher, H.,, Al-Zuhair, S.,, Al-Marzouqi, A.H.,, Haik, Y.,, Farid, M., and Tariq, S., 2014. Supercritical carbon dioxide extraction of microalgae lipid: Process optimization and laboratory scale-up. *The Journal of Supercritical Fluids*, 86, pp.57–66.

Theegala, C.S., 2015. Algal Cell Disruption and Lipid Extraction: A Review on Current Technologies and Limitations. In: A. Prokop, K.R. Bajpai and E.M. Zappi, eds., *Algal Biorefineries: Volume 2: Products and Refinery Design*. Cham: Springer International Publishing, pp.419–441.

Trivedi, J.,, Aila, M.,, Bangwal, D.P.,, Kaul, S., and Garg, M.O., 2015. Algae based biorefinery—How to make sense? *Renewable and Sustainable Energy Reviews*, 47, pp.295–307.

Viêgas, C.V.,, Hachemi, I.,, Freitas, S.P.,, Mäki-Arvela, P.,, Aho, A.,, Hemming, J.,, Smeds, A.,, Heinmaa, I.,, Fontes, F.B.,, da Silva Pereira, D.C.,, Kumar, N.,, Aranda, D.A.G., and Murzin, D.Y., 2015. A route to produce renewable diesel from algae: Synthesis and characterization of biodiesel via in situ transesterification of Chlorella alga and its catalytic deoxygenation to renewable diesel. *Fuel*, 155, pp.144–154.

Wellburn, A.R., 1994. The Spectral Determination of Chlorophylls a and b, as well as Total Carotenoids, Using Various Solvents with Spectrophotometers of Different Resolution. *Journal of Plant Physiology*, 144(3), pp.307–313.

Yang, F.,, Xiang, W.,, Sun, X.,, Wu, H.,, Li, T., and Long, L., 2014. A novel lipid extraction method from wet microalga Picochlorum sp. at room temperature. *Marine drugs*, 12(3), pp.1258–70.

Zhou, L., and Lawal, A., 2016. Hydrodeoxygenation of microalgae oil to green diesel over Pt, Rh and presulfided NiMo catalysts. *Catalysis Science & Technology*.

Zuo, H.,, Liu, Q.,, Wang, T.,, Ma, L.,, Zhang, Q., and Zhang, Q., 2012. Hydrodeoxygenation of Methyl Palmitate over Supported Ni Catalysts for Diesel-like Fuel Production. *Energy & Fuels*, 26(6), pp.3747–3755.

APPENDICES

List of appendices

Appendix 1: Reactor used for supercritical lipid extraction

Appendix 2: Reactor of hydrodeoxygenation experiment

Appendix 1: Reactor used for supercritical lipid extraction

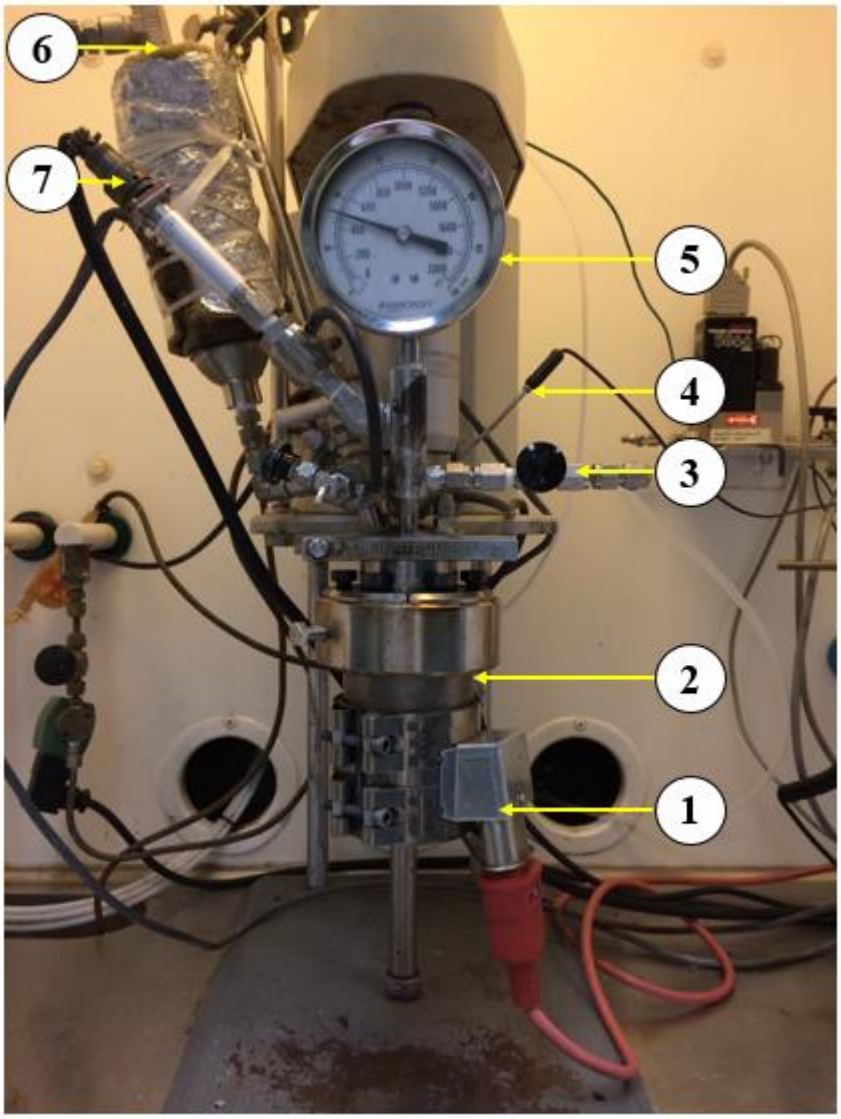

Notation:

1. Heating jacket
2. Reactor
3. Gas out
4. Thermocouple
5. Pressure indicator
6. Gas in
7. Pressure controller

Appendix 2: Reactor used for hydrodeoxygenation experiment

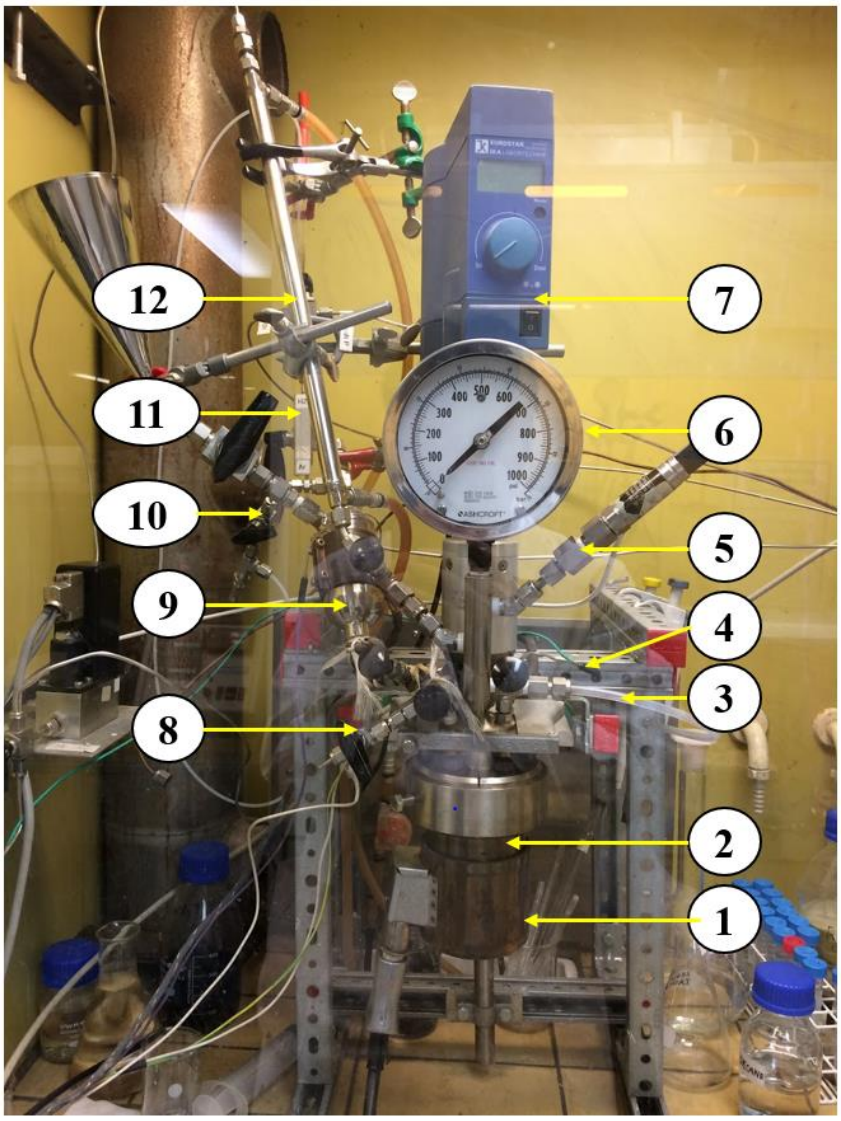

Notation:

1. Heating jacket
2. Reactor
3. Gas out
4. Thermocouple
5. Pressure controller
6. Pressure indicator
7. Stirrer
8. Collector unit
9. Bubbling unit
10. Gas out
11. Gas in
12. Cooler